ISTANBUL TECHNICAL UNIVERSITY ★ GRADUATE SCHOOL

SYNTHESIS OF ZnCdSSe, CdSSeTe QUATERNARY AND ZnCdSSeTe QUINARY ALLOY QUANTUM DOTS VIA TWO PHASE SYNTHESIS METHOD

M.Sc. THESIS

Merve ERKAN

Department of Chemistry

Chemistry Programme

JUNE 2023

ISTANBUL TECHNICAL UNIVERSITY ★ GRADUATE SCHOOL

SYNTHESIS OF ZnCdSSe, CdSSeTe QUATERNARY AND ZnCdSSeTe QUINARY ALLOY QUANTUM DOTS VIA TWO PHASE SYNTHESIS METHOD

M.Sc. THESIS

Merve ERKAN
(509201216)

Department of Chemistry

Chemistry Programme

Thesis Advisor: Assoc. Prof. Caner ÜNLÜ

JUNE 2023

İSTANBUL TEKNİK ÜNİVERSİTESİ ★ LİSANSÜSTÜ EĞİTİM ENSTİTÜSÜ

ZnCdSSe, CdSSeTe DÖRTLÜ VE ZnCdSSeTe BEŞLİ ALAŞIM KUANTUM NOKTACIKLARININ İKİ FAZ SENTEZ YÖNTEMİ İLE SENTEZLENMESİ

YÜKSEK LİSANS TEZİ

Merve ERKAN
(509201216)

Kimya Anabilim Dalı

Kimya Programı

Tez Danışmanı: Doç. Dr. Caner ÜNLÜ

HAZİRAN 2023

Merve ERKAN, a M.Sc. student of ITU Graduate School student ID 509201216 successfully defended the thesis entitled "SYNTHESIS OF ZnCdSSe, CdSSeTe QUATERNARY AND ZnCdSSeTe QUINARY ALLOY QUANTUM DOTS VIA TWO PHASE SYNTHESIS METHOD", which she prepared after fulfilling the requirements specified in the associated legislations, before the jury whose signatures are below.

Thesis Advisor :	**Assoc. Prof. Caner ÜNLÜ** Istanbul Technical University	.....
Jury Members :	**Assoc. Prof. Argun GÖKÇEÖREN** Istanbul Technical University	.....
	Assoc. Prof. Ahmet Emin ATİK Acıbadem University	.....

Date of Submission : 26 May 2023
Date of Defense : 12 June 2023

To my family and my dear fiancé,

FOREWORD

I would like to first thank Assoc. Prof. Caner ÜNLÜ for his guidance and full support. He always kindly guide how to find answers and show how to improve the ideas and projects. Besides his supervisor side, I also want to thank and mention that I learnt a lot from his kindness and his positive communication way. Although I am working for a full-time job, he accepted me to his team and gave me opportunity to complete this thesis. I am deeply thankful and happy to find a chance to work with him.

I thank Dr. Bünyamin KARAGÖZ and Dr. Ahmet GÜL for giving permission to use Fluorescence and UV-Vis spectrometer found in their lab.

I also would like to thank all BeeDot team members, especially Nida ÜK for their valuable support.

I thank my family for their endless support in every phase of my life and I would like to deeply thank to my twin sister Meltem for being always by my side without hesitation and give all her support in every possible way. After working full day, first thing that she asked me when she came home, was 'Did you write your thesis?' and if I said no, she forced me to go outside to a coffee shop and brought me a coffee. While I was studying, she was enjoying her latte and reading a book. This was huge motivation for me.

I also want to thank my dear friend Begüm to encouraged me to start my graduate journey, Oğuzhan and Özge for their enjoyable accompany while I was studying for my exams.

I can not forget how Kerim helped me to synthesize my first quantum dots while I was an undergraduate student. I would like to thank him to introduce me such an exciting research field.

Lastly, I would like to thank my fiancé Sertan to always find how to get over any challenge in my personal and educational life with his kind and unconditional support.

This thesis was supported by Istanbul Technical University – Scientific Research Projects Unit (ITU-BAP) [TYL-2021-43457].

May 2023

Merve ERKAN
(Chemist)

TABLE OF CONTENTS

Page

ABBREVIATIONS

FL	**:** Fluorescence
UV-Vis	**:** Ultraviolet Visible
XPS	**:** X-Ray Photoelectron Spectroscopy
XRD	**:** X-Ray Difractometer

LIST OF TABLES

Page

LIST OF FIGURES

Page

SYNTHESIS OF ZnCdSSe, CdSSeTe QUATERNARY AND ZnCdSSeTe QUINARY ALLOY QUANTUM DOTS VIA TWO PHASE SYNTHESIS METHOD

SUMMARY

Altering the materials' size and reforming them in nano scale provide important scientific enhancements which facilitates invention and development of purpose-oriented technologies. Decreasing the size of the materials to nano scale leads them to gain beneficial and different chemical and physical properties compared to their original form, therefore nanotechnology term became important to improve revolutionary next generation technologies in accordance with human needs.

With the knowledge of the importance of nanotechnology, one of the new nano sized materials called quantum dots becomes popular. Combining generally II-VI and III-V groups of elements found in periodic table while decreasing the size of the compound to 2 -15 nm forms quantum dots [1-3], which have unique optical properties and have great potential to provide important advances in solar cells (Nozik et al., 2010), biosensors (Hakimian et al., 2018), biomedical imagining systems (Mansur et al., 2018), photodetectors (Li et al., 2020), high efficiency LEDs (Pidluzhna et al., 2019), and drug delivery systems. (Ruzycka-Ayoush et al., 2021) [4-9]. Quantum dots are semiconductors, considered as zero-dimensional material and they obey the quantum confinement effect, which is the main reason why quantum dots have great potential to be used in such a wide range of application area. Their zero-dimensional form and having smaller size than their Bohr radius affect their energy bands, found in their conduction and valance band, make them to gain discreet form and this provides several advantages over their original bulk form whose energy band are in continuous form. Discrete form of the energy bands and quantum confinement effect enable quantum dots' optical properties become tunable by changing their size and composition, which leads a change in their band gaps. To understand the effect of the size on optical properties, Brus equation should be considered. (Brus, 1984) [10]. It describes that when size of the quantum dots decreases, their Bohr radius becomes smaller, which is the length of an exciton and exciton can be described as when a photon came, an electron passes through the conduction band, and it is considered that a hole is remained behind in the valance band. This electron and hole pair are called exciton and decreasing the size of the quantum dots causes a decrease in the distance between electron and hole pair while increasing the band gap, which provides the generation of small length of exciton. [1] Smaller length of an exciton requires more energy to separate its electron from its hole by a photon in order that the electron passes to the conduction band. As a result, recombination of electron and hole causes higher energy photon emission compared to the bigger size quantum dots. This is the main reason that decreasing the size of the quantum dots provides blue shift while increasing the size causes red shift in the absorption and the emission of the spectra. The tunability of the band gap by changing size and compositions provides diversity in optical properties of the quantum dots and this explains their importance to the improvements

of the next generation display technologies. In addition, they are known as possessing high quantum yield, it provides signal brightness and helps them to eliminate other signal interferences for the display technology and their high surface to volume ratio makes them also attractive to be able to load more active ingredients for the future applications of the drug delivery systems. [11,12]

The goal of making quantum dots feasible and suitable for the industry and improve their optical properties to expand their application area, synthesis methods are considered as one of the most important parameters, which have direct effect on size and generated quantum dots' type. Over the years, discovered synthesis methods enable to form not only core type quantum dots, which contain one component in their structure but also to form core -shell model and alloyed systems quantum dots, in which there is possibility to have more than one anion and cation in the structure [13,14]. This leads a great enlargement of the research area of the quantum dots and broaden the possibility of taking advantages on different composition features by affecting directly photophysical properties of the quantum dots. Hot injection method for synthesizing quantum dot is one of the most popular synthesis methods. However, it requires high temperatures and high boiling point solvents and dangerous chemicals. Moreover, fast injection is important as temperature to control the monodispersity, shape and size of the obtained quantum dots [15,16]. To enhance the similar defects of the other synthesis methods resembles to the defects of hot injection methods, two phase synthesis methods is discovered [18]. It allows to obtain quantum dots at low temperature 100 0C, which prevents usage of high boiling point solvents and lower the amount of dangerous chemicals. In addition, it provides slow growth, which enables full control over the shape, size and monodispersity of the obtained quantum dots in a more environmentally friendly medium.

To obtain high luminescent quantum dots, cadmium precursors are widely used, and cadmium-based quantum dots are seen to be great candidate for display technology. However, although its high luminescent properties, cadmium toxicity limits the cadmium-based quantum dots usage in biomedical imagining systems and biological technologies. Free cadmium ions cause several damages such as kidney and liver failure while causing cell death on humans and animals, and considered as environmental pollutant [19,20]. In near future, it is expected that Global Environmental Regulations will strictly limit Cadmium usage in next generation display technologies. Therefore, scientists are investigating prevention of releasing cadmium ions from quantum dots structures by applying passivation methods on the surface of the quantum dots and they are trying to reduce the amount of cadmium in the structure.

In this study, with the advantages of two-phase synthesis method and alloyed systems, quaternary alloyed CdSSeTe, ZnCdSSe and quinary alloyed ZnCdSSeTe quantum dots were synthesized to expand and ensure Cadmium-based quantum dots usage in next generation display technologies by decreasing the Cadmium amount in the structure while preserving and improving its current beneficial optical properties. Two strategies were followed to wider the application area of the cadmium-based quantum dots. First one was adding zinc to CdSSe ternary alloyed quantum dots in order to obtain ZnCdSSe, which enabled to lower the cadmium amount in the structure and second strategy was to add tellurium to CdSSe ternary alloyed quantum dots to broad absorption and controllable emission wavelength range. It is also planned to obtain ZnCdSSeTe quinary alloyed quantum dots to achieve the goal of lowering cadmium

amount in the structure and broaden the controllable wavelength of the quantum dots at the same time.

Syntheses were conducted at 100 0C. Toluene used as non-polar phase and distilled water used as polar phase. At the interface between the toluene contained cations and distilled water contained anions, growth of the quantum dots occurred within 3 hours and 24 hours. Zinc stereate (as Zinc precursor) and Cadmium Myristate (as Cadmium precursor) mixed with oleic acid, which was used as surfactant, in toluene phase. Selenium and Tellurium were reduced with sodium borohydride in distilled water to form NaHSe and NaHTe under nitrogen gas to prevent oxidation and added to the polar, distilled water phase. In every determined time frames, adequate amount of the quantum dots, which were passed from the interface to the toluene phase, were taken and their colored emissions, which gives information about the quantum dots' size, controlled by using UV lamp.

To enlighten the composition effect and size on optical properties of the quantum dots, Fluorescence spectrometer and UV-Visible spectrometer were used. Absorption and the emission spectra of the synthesized quantum dots within the time interval 1 hour, 3 hours and 24 hours were obtained. It ensured the slow growth of the quantum dots, which was the main features of the two-phase synthesis method. For the samples collected at 1 hour and 3 hours, the peaks are wide and became sharper for the 24 hours samples. It showed the growth of the quantum dots became stable and 24 hours reaction time reduced the dispersity of the size of the formed quantum dots.

For the structural characterization XRD was used and precipitated quantum dots after 24 hours reaction time was measured. The result showed that Zinc and Tellurium could be added to the ternary alloyed CdSSe structure to form ZnCdSSe and CdSSeTe. However, adding Zinc to the quaternary alloyed quantum dot ZnCdSSeTe could not be achieved, it was found that crystal structure was distorted while forming quinary alloyed quantum dots.

Different amount of Cadmium contained ZnCdSSe quaternary alloyed quantum dots synthesized, and it enabled to understand the importance of the cadmium presence in the structure, and it allowed us to lower the amount of cadmium half of its amount found in CdSSe ternary alloyed quantum dots. In addition, CdSSeTe quaternary alloyed quantum dots synthesized with different ratio of Tellurium resulted to enlarge the absorption and controllable emission wavelength range and with the same amount of the cadmium found in CdSSe ternary alloyed quantum dots, which has blue color could be shift to the yellow with a great shift observed in the spectra.

ZnCdSSe, CdSSeTe DÖRTLÜ VE ZnCdSSeTe BEŞLİ ALAŞIM KUANTUM NOKTACIKLARININ İKİ FAZ SENTEZ YÖNTEMİ İLE SENTEZLENMESİ

ÖZET

Malzemelerin boyutlarının değiştirilmesi ve nano ölçekte yeniden biçimlendirilmesi, amaca yönelik teknolojilerin icat edilmesini ve geliştirilmesini kolaylaştıran önemli bilimsel gelişmeler sağlamaktadır. Malzemelerin boyutlarının nano ölçeğe düşürülmesi, orijinal yapılarına göre gelişmiş kimyasal ve fiziksel özellikler kazanmalarına yol açarak devrim niteliğindeki yeni nesil teknolojilerin insan ihtiyaçlarına uygun olarak geliştirilmesinde önemli katkılara öncü olup nanoteknoloji teriminin önem kazanmasını sağlamıştır.

Nanoteknolojinin önem kazanması ile birlikte boyutları 2-15 nm aralığında bulunan yarı iletken kuantum noktacıkları da yeni nesil teknolojilerin geliştirilmesi adına benzersiz optik ve foto-fiziksel özellikleriyle önemli bir aday olarak görülmüş olup, foto detektörler, QLED olarak adlandırılan yüksek verimli LED'ler, biyomedikal görüntüleme sistemleri, ilaç iletim sistemleri gibi birçok farklı alanda kullanım alanlarına katkı sağlamaktadır.

Genellikle periyodik tablonun II-VI ve III-V grup elementlerinden oluşan kuantum noktacıklarının üstün optik özellikleri Bohr uyarım yarıçapları ve kuantum sınırlaması etkisi nedeniyle boyuta bağlı optik özelliklerinin kontrol edilebilmesinden kaynaklanmaktadır. Bu nedenle hedeflenen kullanım alanına göre kuantum noktacıklarının optik özelliklerinin değiştirilebilmesi kuantum noktacıklarına geniş bir uygulama alanı potansiyeli sunmaktadır.

Bohr uyarım yarıçapından küçük olan boyutları kuantum noktacıklarının değerlilik ve iletkenlik bantlarında bulunan enerji seviyelerinin orijinal formlarındaki hallerine göre sürekli değil ayrık halde bulunmasını sağladığından, kuantum sınırlama etkisine uyarak boyuta bağlı optik özelliklerinin değiştirilebilmesi özelliğine sahip olmasına neden olur. Değerlilik bandı ile iletkenlik bandı arasındaki bant boşluğu, boyut değişikliği ile değiştirilebildiğinden kuantum noktacıklarının boyutlarının değişmesi farklı emisyon dalga boylarının elde edilebilmesini sağlar. Uyarım sonucu değerlilik bandından iletkenlik bandına geçen elektronun arkasında bir boşluk bıraktığı düşünülür. Bu elektron ve boşluk çiftine eksiton denir. Elektron ve boşluk çiftinin arasındaki uzaklık ise kuantum noktacıklarının boyutu azaldıkça azalır ve uyarım sonucu elektronun değerlilik bandından iletkenlik bandı arasındaki kat etmesi gereken uzunluk yani bant boşluğu artar. Bu nedenle boyutu küçük olan kuantum noktacıkları büyük olan kuantum noktacıklarına göre daha yüksek enerjili uyarım ile elektronlarının iletkenlik bandına geçebilmesi sağlanacağından, elektronun iletkenlik bandından değerlilik bandına dönerek boşluk ile tekrar birleşmesi sonucunda daha büyük boyutlardaki kuantum noktacıklarına göre daha yüksek enerjili emisyona neden olur. Bu nedenle emisyon spektrumunda kuantum noktacıklarının boyutları azaldıkça daha yüksek enerjili ve daha düşük dalga boylu ışıma gözlemlenir. Bu nedenle kuantum noktacıklarının boyutlarının artması kırmızı bölgeye doğru emisyon dalga boylarında bir kaymaya neden olarak boyuta bağlı optik özelliklerinin ayarlanması ile

görünür bölgede tüm frekanslarda ışıma elde edilmesi sağlanabilmektedir. Geniş emisyon spektrumu ile yüksek kuantum verimi özellikleri kuantum noktacıklarını görüntüleme teknolojilerinde önemli bir aday olmasını sağlar. Yüksek yüzey alanı ve hacim oranı ilaç iletim sistemlerinde etken maddenin yüksek oranda depolanmasının önünü açarak bu alanda önemli bir potansiyele sahip olmasını sağlamaktadır.

Sentez yöntemi kuantum noktacıklarının boyutuna, şekline, türüne dolayısıyla optik özelliklerine olan direk etkisi nedeniyle kuantum noktacıklarının amaca yönelik teknolojilerde kullanım alanlarını arttırabilmek ve büyük ölçekli üretime uygun hale getirebilmek için en önemli parametre olarak görülmektedir. Bu nedenle birçok sentez yöntemi keşfedilmiştir. Keşfedilen sentez yöntemleri ile elde edilen kuantum noktacıklarının optik özelliklerinin geliştirilmesini sağlamak amacıyla birçok farklı tür kuantum noktacıkları elde edilmiştir. Bu sentez yöntemleri ile yapılarında sadece tek bir bileşen bulunan kuantum noktacıklarının yanı sıra birden fazla anyon ve katyonun bulunma olasılığının bulunduğu çekirdek-kabuk modeli geliştirilmiştir. Bu model ile kuantum noktacıklarının yüzeyinde bulunan kusurlar, oluşturulan kabuk ile giderilerek yüzey pasivasyonu sağlanmış olur ve bu nedenle kabuk stabilitenin ve kuantum veriminin artmasında önemli bir görev görerek tek bileşenli kuantum noktacıklarının optik özelliklerinin geliştirilmesini sağlar. Bu modelin yanı sıra alaşım sistemli kuantum noktacıkları oluşturulmuş olup üçlü, dörtlü ve beşli alaşım sistemleri oluşturularak çoklu katyon ve anyon içeren kuantum noktacıkları ile çekirdek- kabuk modelindeki gibi yüzey kusurlarının giderilmesi aynı zamanda sadece boyuta bağlı değil kompozisyona bağlı optik özelliklerinin değiştirilebilmesi amaçlanarak kuantum noktacıklarının kullanım alanlarının genişlemesi adına önemli bir adım atılması sağlanmıştır.

Sıcak enjeksiyon yöntemi kuantum noktacıklarının en yaygın sentez yöntemlerinden biridir. Bu yöntem ile kuantum noktacıkları, katyon ve yüzey aktif madde içeren yüksek sıcaklıklardaki reaksiyon ortamına hızlı soğutulmuş anyon içeren solüsyonun enjekte edilmesi ile elde edilir. Kuantum noktacıkları enjeksiyon sonrası saniyeler içerisinde oluşur. Enjeksiyonun hızı ve reaksiyon ortamının sıcaklığı oluşan kuantum noktacıklarının boyutuna, şekline ve homojenliğine direk etki ettiğinden istenilen özellikte kuantum noktacıklarının elde edilmesi yavaş büyüme sağlayan sentez yöntemlerine göre zordur. Bu sentez yöntemi yüksek sıcaklık gerektirdiğinden Oktadesen, TOP ve TOPO gibi kaynama noktası yüksek, tehlikeli ve çevreye zararlı çözücüler kullanılmasını gerektirir.

Bu nedenle iki faz sentez yöntemi sıcak enjeksiyon ve benzer sentez yöntemlerinin çevreye zararının azaltılabilmesi ve elde edilen kuantum noktacıklarının boyutu, şekli ve homojenliği üzerindeki tam kontrolü, kuantum noktacıklarının yavaş büyüme hızı ile sağlamak için keşfedilmiş olup, bu yöntem yüksek sıcaklık gerektirmediğinden kaynama noktası yüksek çözücü kullanımı azaltılmış ve yavaş büyüme hızı ile sentezlenen kuantum noktacıkları üzerinde tam kontrol sağlanarak sıcak enjeksiyon ve benzer sentez yöntemlerinin olumsuz özelliklerinin amaca yönelik geliştirilmesi sağlanmıştır. Bu sentez yöntemi düşük sıcaklıkta sadece tekli sistemlerin değil alaşım sistemleri içinde uygun bir sentez yöntemi olup kuantum noktacıklarının yavaş oluşma hızı eklenen prekürsörlerin çözünürlük ve reaktivitelerinin kontrol edilerek alaşım sistemli kuantum noktacıkların elde edilmesini kolaylaştırır. Bu yöntemde katyon kaynağı, genellikle oleik asit yüzey aktif maddesi ile tolüen içerisinde çözünür ve belirlenen sıcaklıktaki suda çözünmüş anyon kaynağını içeren faza eklenir. Oluşan kuantum noktacıkları ara fazdan tolüen fazına geçer ve bu fazdan polar çözücü ile çöktürülerek elde edilir.

Yüksek ışıma yapan kuantum noktacıkları için kadmiyum en yaygın kullanılan elektropozitif maddedir, kadmiyumun sağladığı avantajlar nedeniyle kadmiyum tabanlı kuantum noktacıkları görüntüleme teknolojilerinde önemli bir aday olarak görülmektedir. Fakat kadmiyum, kuantum noktacıklarına yüksek kuantum verimi, parlaklık ve gelişmiş optik özellikleri sağlamasına rağmen yüksek toksisitesi nedeniyle biyomedikal görüntüleme alanında kullanım potansiyelleri sınırlıdır. Serbest kadmiyum iyonları hücre ölümüne neden olarak insan sağlığına ve çevreye ciddi zararlar verdiğinden, kadmiyum iyonlarının yapıdan ayrılmasını engellemek amacıyla yüzey pasivasyon metotları araştırılmaktadır. Yakın gelecekte kadmiyum kullanımının kullanım alanı fark etmeksizin global çevre regülasyonlarına göre ciddi sınırlamalar getirileceği düşünülmekte olduğundan araştırmalar, kadmiyumun sağladığı optik avantajları yapıdaki kadmiyum oranını azaltarak koruma amacıyla geliştirilen çeşitli yöntemler üzerinde yoğunlaşmaya başlamıştır.

Bu nedenle bu tezin ana amacı, iki faz sentez yönteminin sadece boyuta bağlı değil kompozisyona bağlı optik özelliklerinin geliştirilmesine imkan tanıyan alaşım sistemli kuantum noktacıklarının elde edilmesindeki avantajını kullanarak CdSSe üçlü alaşım sistemli kuantum noktacıklarının yapısında bulunan kadmiyum miktarını çinko ekleyerek azaltarak dörtlü alaşım sistemli ZnCdSSe kuantum noktacıkları elde etmek olup, kadmiyum tabanlı kuantum noktacıklarının gelecekteki kullanım potansiyellerini geliştirmektir. Bu tezde aynı zamanda üçlü alaşım sistemli CdSSe kuantum noktacıklarının kontrol edilebilir emisyon spektrumunun genişletilmesini yapıya tellür eklenmesiyle CdSSeTe dörtlü alaşım sistemli kuantum noktacıklarının elde edilmesini sağlayarak orijinal CdSSe kuantum noktacıklarının kullanım alanlarının arttırılması amaçlanmıştır. Bu iki amacın aynı anda elde edilebilmesi için üçlü alaşım sistemli CdSSe kuantum noktacıklarının yapısına hem çinko hem tellür eklenmesi denenerek çinkonun kadmiyum miktarının azaltılmasındaki etkisi ile birlikte aynı zamanda tellür eklenmesi gerçekleştirilerek beşli alaşım sistemli ZnCdSSeTe kuantum noktacıkları elde edilmesi denenerek üçlü CdSSe ve dörtlü ZnCdSSe yapılarının kontrol edilebilir emisyon spektrumunun genişletilmesi ile aynı anda yapıdaki kadmiyum oranının azaltılması hedeflenmiştir.

Bu çalışmada kuantum noktacıkları elde edilirken, kadmiyum ve çinko katyon kaynağı olarak kadmiyum miristat ve çinko stearat kullanılmış olup tolüen fazında yüzey aktif madde olan oleik asit ile birlikte çözünmüştür. Selenyum ve tellür kaynağı olarak sodyum borhidrür solüsyonu ile tellür ve selenyum indirgenmiş ve azot ortamında sülfür kaynağı olan tiyoüre içeren su fazına 100 ^{0}C' de eklendikten sonra katyon içeren tolüen fazı eklenmiştir. Reaksiyon süresi her sentez için 24 saat olarak belirlenmiş ve belirlenen aralıklarda ara fazda oluşarak tolüen fazına geçen kuantum noktacıkları bu fazdan toplanarak elde edilen kuantum noktacıklarının büyümesi UV ışık altında ve floresan spektrometre ile kontrol edilmiştir. Reaksiyon 24 saatin sonunda durdurulduğunda tolüen fazı ve su fazı birbirinden ayrılarak tolüen fazı filtreden geçirilmiş ve 1:1 oranda metanol eklenerek kuantum noktacıklarının çöktürülmesi sağlanmıştır. Elde edilen kuantum noktacıklarının optik özellikleri, 366 nm UV ışığı, floresan spektrometre kullanarak emisyon ve eksitasyon spektrumları, UV spektrometre ile de absorbsiyon spektrumları elde edilerek ölçülmüş. Yapısal karakterizasyonları ise X-RAY Difraktometre ile ölçülmüştür.

Üçlü alaşım sistemli CdSSe kuantum noktacıklarının yapısına farklı oranda Tellür eklenmesi ile birlikte dörtlü alaşım sistemli CdSSeTe kuantum noktacıkları elde edilmiş olup modifiye edilerek dörtlü sisteme dönüştürülmüş CdSSe kuantum noktacıklarının kontrol edilebilir emisyon spektrumunun genişletilmesi sağlanmıştır.

Eklenen Tellür miktarı arttıkça mavi renk ışıma yapan CdSSe kuantum noktacıkları CdSSeTe yapısına dönüştürülmesi ile eklenen Tellür miktarının arttırılmasıyla sarı renkli ışıma elde edilebilmiştir. Absorbsiyon ve emisyon spektrumları ile bu kırmızı bölgeye kayma kaydedilmiştir. CdSSe kuantum noktacıklarının eksitasyon spekrumları ile XRD sonuçları elde edilen CdSSeTe kuantum noktacıkları ile karşılaştırılarak yapıya tellür katılımının gerçekleştiği kanıtlanmıştır.

Daha sonrasında üçlü CdSSe yapısına Çinko eklenerek ZnCdSSe yapısı elde edilmiş ve belirli çinko oranında CdSSe yapısında bulunan Kadmiyum miktarı Çinko eklemesi ile yarı yarıya düşürülerek alaşım sisteminin avantajı ile birlikte kadmiyum oranının çinko eklemesi ile azaltılması sağlanmasının yanı sıra bu değişim ile mavi ışıma yapan CdSSe kuantum noktacıklarının kontrol edilebilir emisyon spektrumunun genişletilmesi elde edilen ZnCdSSe yapısının yeşil ışıma yapması ile sağlanmış olup kadmiyum oranını azaltmak ve kontrol edilebilir emisyon spektrumunu genişletme amacına aynı anda ulaşılabilmiştir. Yapıya çinko katılımı CdSSe ve ZnCdSSe kuantum noktacıklarının XRD ve eksitasyon spektrumu ile gözlemlenmiş olup mavi ışıma yapan CdSSe kuantum noktacıklarının yapısına belirli oranda çinko eklenmesi maksimum absopbsiyon ve emisyon dalga boyunun kırmızı bölgeye doğru kayması UV ve floresans spektrometresi ile gözlemlenmiştir.

Fakat üçlü sisteme hem çinko hem tellür eklenerek bu iki amacın aynı anda beşli alaşım sistemli ZnCdSSeTe yapısı ile elde edilmesi sağlanması mümkün olmamıştır. Yapısal karakterizasyondan elde edilen sonuçlar beşli alaşım sisteminin üçlü CdSSe yapısına çinko ve tellür katılımı ile oluşturulmasının sağlanamadığını kanıtlamıştır.

1. INTRODUCTION

1.1 Quantum Dots

Quantum dots' discovery in 1981 by Ekimov and Onushenko was considered as one of the most groundbreaking and revolutionary discovery of 20th century because of their incomparable and promising optical properties [1]. With the first discovery of the quantum dots researchers focused on investigating the source of their unique optical properties. The relation between the size of the quantum dots and their optical properties formulated and explained in depth first by Louis Brus in 1984 [10]. The researchs started to speed up with an understanding of the importance of size-dependent emission property of quantum dots, which provides wide application potential, included next generation display technologies, bio-imagining system, highly efficient LEDs (QLEDs), drug delivery systems, photodetectors, solar cells [12].

It is found that the main reason of such a wide range of their application area is arise from ultra-small size of the quantum dots, which is between the range of 2-15 nm. They are zero-dimensional, highly fluorescent semiconductors contain 10-10.000 atoms and formed generally II-VI and III-V group of elements found in periodic table [1]. Their ultra-small size compared to their Bohr radius and being zero-dimensional makes them to obey quantum confinement effect, which make their energy bands differ from their bulk form and gains them superior optical properties by leading them to be called as artificial atoms [1,21]. Main difference of their energy bands of the quantum dots are being in discrete form while in bulk form energy bands are found in continuous form (Figure 1.1).

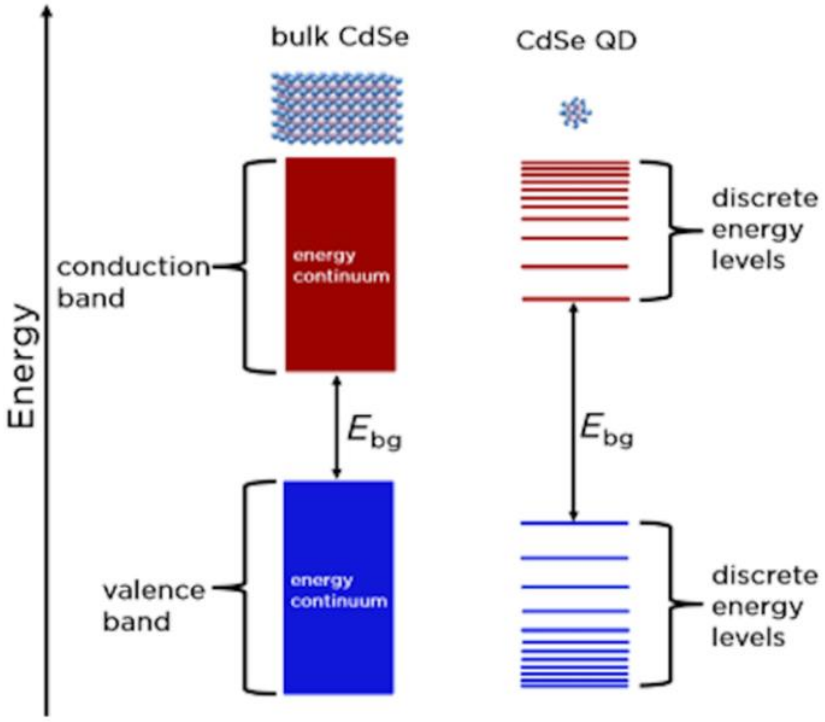

Figure 1.1 : Bulk CdSe and CdSe quantum dots energy bands comparison [22].

Discrete form of the energy bands and quantum confinement effect are the main reason of size-dependent emission property by providing the ability of tunable band gap not only by changing composition but also by changing particle size of the quantum dots [23]. To understand the relation of the size and emission of the quantum dots, Brus equation should be considered [10]. It describes the relation between the size and exciton Bohr radius with a concept of energy bands. When a photon excites an electron and causes its transfer to the conduction band, a hole is considered to be left in the valance band [24]. It is considered there is an attraction between this electron and hole and this electron and hole pair called exciton. The similarity of the electron and hole, with electron and nucleus found in a hydrogen atom makes the distance between the electron and hole pair called as exciton Bohr radius and this distance decreases when the size of the quantum dots decreases and the energy band between its conduction band and the valence band increases [25]. To overcome the attraction of this electron and hole pair and to pass the distance between valance and conduction band makes more difficult to separate the electron from hole and reach the electron to the conduction band, therefore it requires more energy to transfer electron to the conduction band compared to the bigger size of the quantum dots [26]. Since the band gap between the conduction and valance band is greater than the bigger size quantum dots, the radiative recombination of the electron and hole in the valance band causes

emission of a photon, which is higher in frequency and lower in wavelength [27]. Therefore, changing the composition is not the only option to alter the band gap, size becomes another parameter to provide various color of emission to the quantum dots (Figure 1.2).

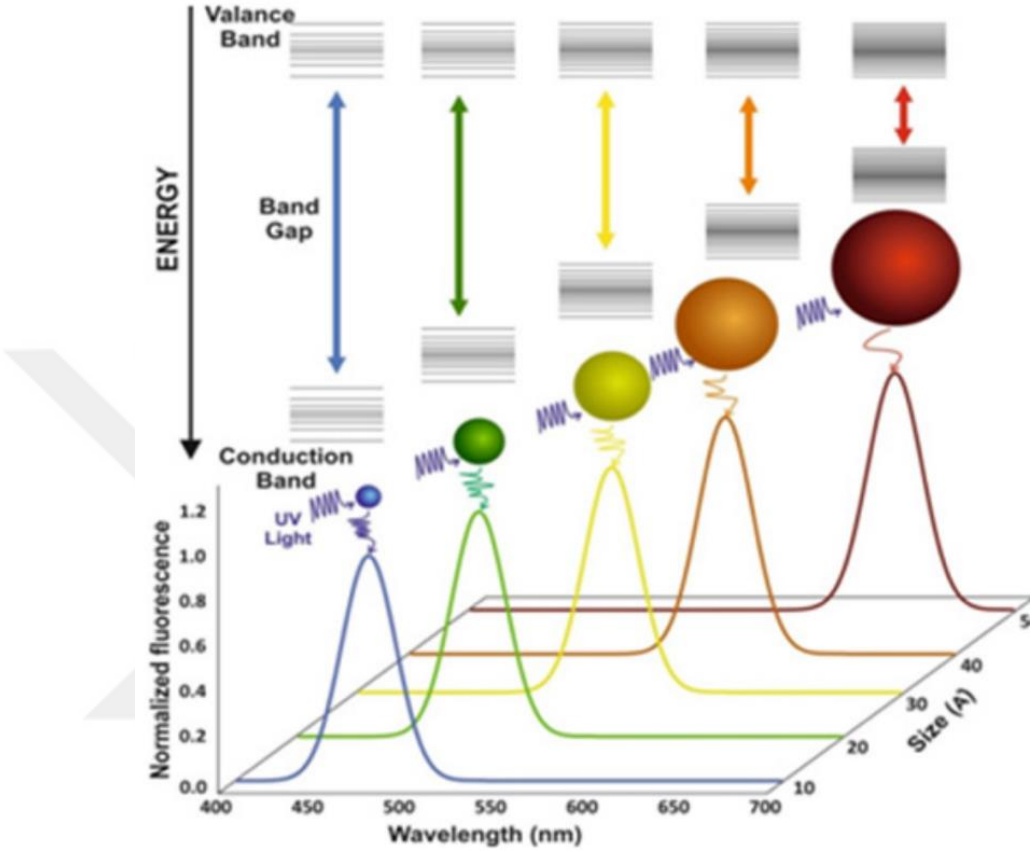

Figure 1.2 : Size-dependent emission property of the quantum dots [28].

1.2 Type of Quantum Dots

Combination of one chalcogens such as selenium, tellurium, and sulfide with one electropositive material such as cadmium form common core type of binary quantum dots. Their optical properties can be changed only by changing the particle size and their absorption and controllable emission wavelength range is limited with the size change. Quantum dots have high surface to volume ratio; therefore, their fluorescence quality depends highly on the surface defect states because surface defect states cause internal energy bands (trap states) found between the valance band and conduction band of the quantum dots and it leads non radiative recombination of the excited electron and hole at the defect energy bands found between the valance and conduction band while excited electron turning back to the valance band from the conduction band

[29]. As a result, these defects (trap states) decrease the quantum yield, which describes the efficiency of the transferring absorbed energy to the emitted energy, and the fluorescence of the quantum dots decreases [30]. To overcome these surface defects, passivation methods for the surface are investigating, which can be achieved by changing long alkyl chains found at the surface of the quantum dots with determined ligands by various ligand exchange methods [31].

These researchs of the passivation methods become the source of the generation of the new quantum dot type, which is core-shell type quantum dots. In the core-shell system, the differences of the energy bands between the core and shell results four different types of the quantum dots, which are Type I, Inverse type I, Type II, and Inverse type II [32]. In these four types, Inverse type I provides the desired passivation of the surface of the core because conduction and valance band of the shell is located above both conduction and valance band of the core, which prevents the trap states form within the energy bands of the core and it enables to preserve the quality of the fluorescence of the quantum dots. Since the core energy bands found between the energy bands of the shell, altering the shell band gap by changing its thickness, which can be considered as altering the size of the quantum dots, provides various emission wavelengths by causing the change the distance found between its valance and conduction band [32,33]. Moreover, when energy bands of the shell are found within the energy bands of the core, quantum dots become belong to the type I. If only the conduction band of the quantum dot is found within the energy bands of the shell, it is called type II and the opposite case that only valance band of the core is found within the energy bands of the shell, it is called inverse type II (Figure 1.3) [32-36].

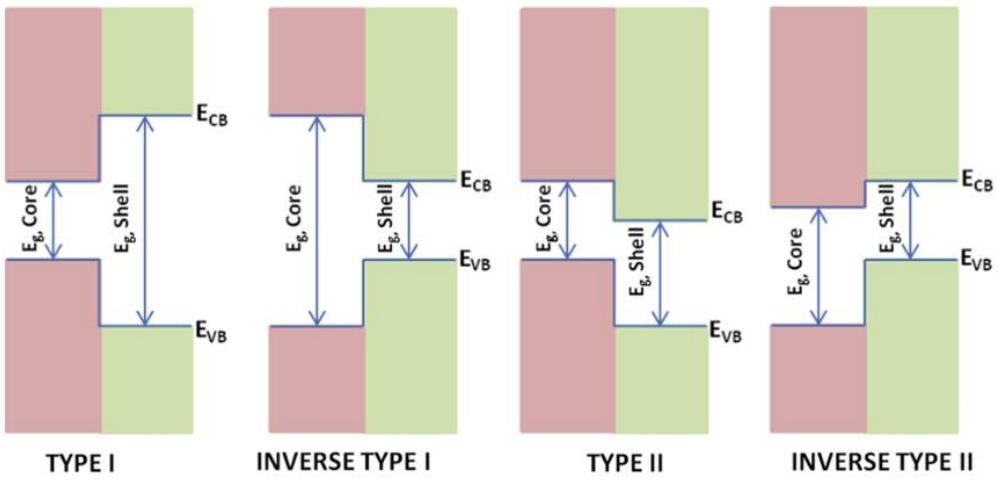

Figure 1.3 : Types of core-shell quantum dots [35].

The main goal of generating highly luminescent quantum dots while expanding the absorption and controllable emission of the quantum dots in order to broaden their application area leads improvement of another type of quantum dots, which can be formed by alloying the core to turn regular binary quantum dots to ternary, quaternary and quinary alloyed systems. Alloyed quantum dots are classified according to their internal structure, when they possess homogeneous internal structure, they are called homogeneous alloyed quantum dots. However, the gradient internal structure can be resembled to core-shell system in which inner core can be rich in particular components and while going to the outer part of the core, the component which is high in the amount can be radiantly change. In this case they are called gradient alloyed quantum dots and their main difference with the core-shell structure is not having strict separation which can be described as shell and in which gradient change can be observed while going from inner part of the quantum dots to the outer part (Figure 1.4) [31,36].

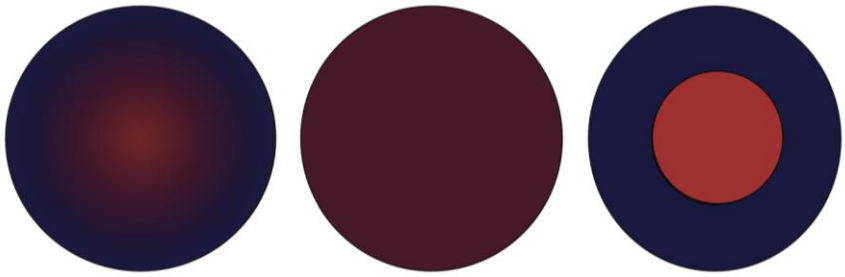

Figure 1.4 : Representation of the alloyed quantum dots and core-shell quantum dots structure [37].

Alloyed systems provide not only enhancement of the surface defects but also enlargement of wavelength range of absorption and controllable emission spectra by not only altering the particle size but also changing the composition of the quantum dots. Since in this type of quantum dots, the size is not the only parameter that affects the emission spectra, composition of the quantum dot becomes another important parameter to alter the band gap of the quantum dots. [14,38]. In fact, this provides alloyed systems to have superior property compared to the same size core type and core-shell structured quantum dots because of their tunable energy bands without changing the particle size. Moreover, there is various combination of compositions to form alloy systems, which also leads their application potential becomes wider in next generation technologies. Having more than one cation or anion in the structure causes

distorted energy bands to alloyed quantum dots because of the differences between the energies of the combined components while changing the regular discrete form of the energy bands found in core and core-shell type quantum dots This phenomenon is called optical bowing and this provides non-linear relation between the composition and the energy emitted with the recombination of the electron and hole [14,39]. It is the key reason why this system enables quantum dots' emission wavelength range becomes wider compared to same size of the core and core-shell structured quantum dots. The importance of the tunable band gap without changing the particle size can be more significant particularly in biological application because in biological systems, particle size determines the passage of the components to the desired targeted area and obtaining superior optical properties without changing particle size gain alloyed system wider application area in biological application [37,40].

1.3 Cadmium-Based Quantum Dots Synthesis Methods

Cadmium is among the most advantageous cation to form chalcogenide quantum dots by gaining quantum dots high luminescent properties and high quantum yields. Therefore, cadmium based quantum dots are one of the most investigating types of quantum dots and generally, they are synthesized with bottom to top approach, to which popular hot- injection synthesis method and two-phase synthesis method can be given as examples.

1.3.1 Hot-injection synthesis method

This synthesis method is the most popular synthesis method to obtain cadmium-based quantum dots because it provides fast growth of quantum dots. In this method, reaction starts with rapid injection of cooled anion precursors into the cadmium precursor media, where temperature is kept generally 300 ^{0}C. Temperature control is the key parameter to obtain desired shape and size of the quantum dots. Since the reaction and growing of the quantum dots occur within seconds (Figure 1.5), size dispersity is highly dependent on the fast injection and terminating time of the reaction by decreasing rapidly the temperature of the media. Highly elevated temperature brings the requirement of the usage of high boiling point, dangerous solvents such as TOP, TOPO and octadecene [15,16,41,42]. Therefore, it leads investigation of other greener and environmentally friendly syntheses methods to continue while eliminating the

disadvantages of the fast growth of the quantum dots, which makes this method difficult to end up with monodisperse quantum dots.

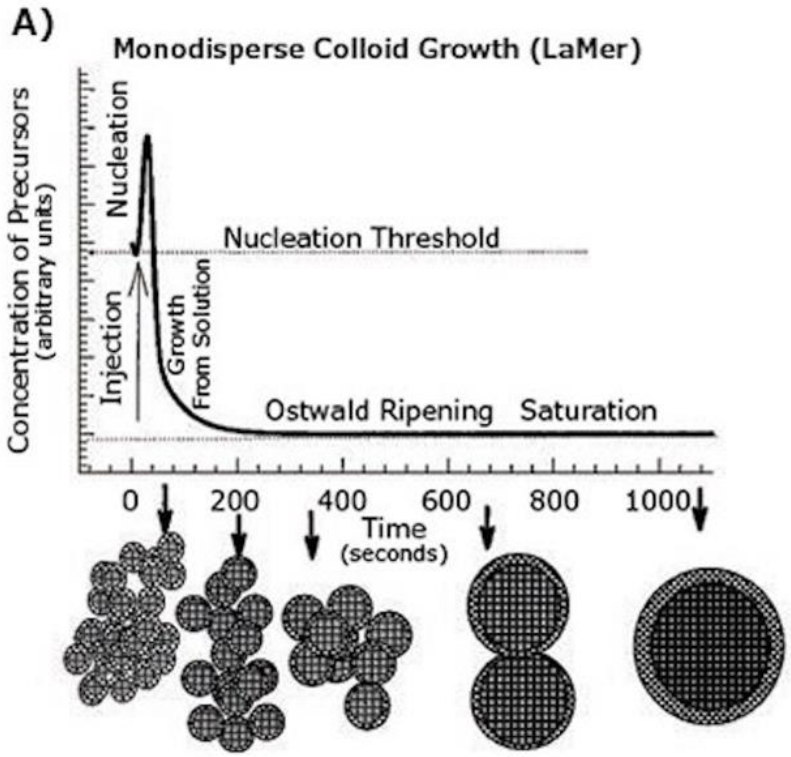

Figure 1.5 : Representation growth of quantum dots with hot-injection synthesis method [42].

1.3.2 Two - phase synthesis method

This synthesis method is excellent alternative to other common synthesis methods when slow growth of the quantum dots is needed to be able to have full control over the obtained quantum dots' size and full control of the dispersity of the obtained quantum dots. This method is designed by Caner Ünlü et al. in 2013 with bottom to top approach and it decreases the usage of high boiling point, dangerous solvents by lowering the reaction temperature to 100 ^{0}C and becomes more environmentally friendly alternative [18]. This synthesis method is not only suitable to form core type quantum dot, but also very advantageous to form alloyed system quantum dots. Because slow growth of the quantum dots enables to take advantages of the reactivity differences of the added precursors, which is significant factor for obtaining alloyed system quantum dots with a gradient internal structure.

In this synthesis method, cation precursors are mixed with oleic acid as surfactant in toluene and quantum dots are obtained from the reaction occurred between the

interface of the water phase contained anion precursor and toluene phase contained cation precursors by providing the interaction of the phases in one pot at 100 ^{0}C [18].

1.4 Toxicity of Cadmium-Based Quantum Dots

Toxicity of the cadmium-based quantum dots can be related mainly with the release of Cd^{+2} ions from the structure because free cadmium ions are considered as toxic to human health and environment. Although it does not have genotoxic features, it is categorized as cytotoxic since it causes severe damage to the DNAs and resulting the cell death. Therefore, free cadmium ions are classified as dangerous pollutant to the environment and hazardous for human health. Exposure of the free cadmium ions causes several vital organs failure with the cell death and therefore exposure of elevated dose should be prevented [43]. In this aspect, it is expected that in near future global environmental regulations will strictly limit the usage of cadmium in next generation display and biomedical imagining technologies. To expand and ensure the usage of the cadmium-based quantum dots especially *in vivo* biological application, core-shell systems are widely investigating because it covers the surface of the cadmium contained core with a non-cadmium included shell and prevents the release free cadmium ions outside to the system [19,43,44]. It enables to protect current beneficial optical properties of the cadmium-based quantum dots while lowering the toxicity. Other passivation methods with ligand exchange methods are also used to eliminate the risk of the release of cadmium ions while turning the hydrophobic quantum dots to soluble in aqueous phase to make them suitable for *in vivo* systems.

2. MATERIALS AND SYNTHESIS

2.1 Materials

Cadmium oxide (CdO, 99.9%, Aldrich), myristic acid ($C_{14}H_{28}O_2$, 99.9%, Aldrich) and toluene ($C_6H_5CH_3$ 99.9%, Aldrich) were used to obtained cadmium myristate precursor.

For synthesizing alloyed quantum dots cadmium myristate, zinc stereate ($C_{36}H_{70}O_4$, technical grade, Aldrich), sodium borohydrate ($NaBH_4$, 98,0%, Merck), selenium powder (100 mesh, 99.5%, Aldrich), tellurium powder (200 mesh, 99.8%, Aldrich), thiouerea (CH_4N_2S, 99.0%, Merck), Oleic Acid (OA, 90%, Aldrich), toluene ($C_6H_5CH_3$, 99.9%, Aldrich), distilled water were used [17].

2.2 Synthesis

Toxicity of the cadmium and the possibility of limitation of cadmium-based quantum dots in near future led this study to form ZnCdSSe, CdSSeTe quaternary and ZnCdSSeTe quinary alloyed quantum dots via advantageous two-phase synthesis methods to form alloyed structures (Caner Ünlü et al. 2013) [17,18]. First strategy was adding zinc into the ternary alloyed quantum dots to lower the cadmium amount found in the structure and second strategy was adding Te into the CdSSe ternary alloyed quantum dots to expand its potential application area with broaden the absorption and controllable emission wavelength range. Lastly, the possibility of adding both zinc and tellerium into the CdSSe ternary alloyed quantum dots was investigated to form ZnCdSseTe quinary alloyed quantum dots in order to combine the advantages of lowering cadmium amount in the structure and wider the emission spectra to increase the potential of the application area of CdSSe ternary alloyed quantum dots.

2.2.1 Preparation of precursor solutions

2.2.1.1 Synhesis of cadmium myristate as cadmium precursor

Synthesis of the cadmium myristate was done according to Pan et al. published method [45]. 1 mole of cadmium oxide was mixed with 2 mole myristic acid at 210 ^{0}C. The reaction was stopped when oxygen outcome completed, and clear solution obtained. White colored precipitation was collected after the reaction temperature drop to room temperature and recrystallized in toluene. Obtained white solid was dried at 50 ^{0}C and for future use stored at 4 ^{0}C in refrigerator [45].

2.2.1.2 Preparation of NaHSe solution as selenium precursor

NaHSe solution was prepared freshly before every synthesis. First, in 10 mL distilled water mixed with 15 mg sodium borohydride ($NaBH_4$, 0,40 mmol) while nitrogen gas passed through the solution about 15 min and it was injected onto selenium powder (10 mg, 0,13 mmol) found previously nitrogen gas filled flask. After stirring at 90 ^{0}C clear solution was obtained and it became ready to use.

2.2.1.3 Prepataion of NaHTe solution as tellurium precursor

NaHTe solution was prepared freshly before every synthesis. $NaBH_4$ solution prepared by mixing 10 mL distilled water and 15 mg sodium borohydride ($NaBH_4$, 0,40 mmol) while nitrogen gas passed about 15 min. Then the solution was injected into 25 mg tellurium powder contained and nitrogen gas filled flask. NaHTe solution obtained when dark violet colored solution observed while stirring at 120 ^{0}C.

2.2.1.4 Synthesis of CdSSe ternary alloyed quantum dots

CdSSe ternary alloyed quantum dots were used as blank material in this study in order to comprehend the effect of composition on optical and structural properties while introducing to cation (Zn) and anion (Te) into the CdSSe ternary alloyed quantum dots' structure to obtain quaternary and quinary alloyed quantum dots.

To obtain CdSSe ternary alloyed quantum dots, 40 mL distilled water and 60 mg thiourea as sulfur precursor (0,79 mmol) were mixed at 100 ^{0}C in 250 mL nitrogen gas filled three-necked round bottom flask. 2 mL freshly prepared NaHSe solution was added into the reaction balloon and immediately after adding NaHSe solution, 0.2 g cadmium myristate as cadmium precursor dissolved in 50 mL toluene with 1.50 g

Oleic Acid (5.3 mmol) poured into the reaction balloon and reaction refluxed under nitrogen gas at 100 ^{0}C. Quantum dots started to form at the interphase of the toluene and water phase and while growing, they passed to the toluene phase because surface of the quantum dots was covered with long alkyl chains came from oleic acid surfactant and they become soluble in toluene phase. Reaction temperature was kept at 100 ^{0}C until synthesis was completed.

Adequate amount of growing quantum dots, which was found in toluene phase, were taken from the reaction mixture between the time interval 5 min, 15 min, 30 min, 1h, 1h 30 mi., 2h, 2h 30 min, and 3h. After 24 hours reaction was stopped by turning off the temperature and water phase and toluene phase were separated with using separation funnel and after toluene phase filtered, quantum dots were obtained by precipitating them with methanol. Precipitated quantum dots were kept in the same solution in 2-8 ^{0}C refrigerator.

2.2.2 Synthesis of CdSSeTe quaternary alloyed quantum dots

Same synthesis procedure of CdSSe ternary alloyed quantum dots was followed, However, in this time, the main differences was adding freshly prepared NaHTe solution after injecting constant amount of 2 mL freshly prepared NaHSe solution into main reaction balloon where 40 mL distilled water and 60 mg thiourea (0,79 mmol) as sulfur precursor found. Immediately after the addition of anion precursors cadmium myristate solution in toluene phase was poured to form CdSSeTe quaternary alloyed quantum dots. Adequate amounts of samples were extracted from reaction balloon within the same determined time intervals as CdSSe QDs synthesis and reaction was stopped after 24 hours. After the filtration and the separation of toluene phase from water phase, quantum dots were precipitated by methanol. Table 2.1 found below shows the used amounts of precursors in this study to understand the effect of composition on formed quantum dots' optical and structural properties.

Table 2.1 : Used precursors' amounts to synthesize CdSSeTe.

Synthesis Code	Cd Myristate	NaHTe solution / Te content	NaHSe solution/ Se content	Thiourea
13_ME_CdSSeTe	0,2 g	2 mL / 5 mg	2 mL / 2 mg	60 mg
16_ME_CdSSeTe	0,2 g	4 mL / 10 mg	2 mL / 2 mg	60 mg
21_ME_CdSSeTe	10 mg	2 mL / 5 mg	2 mL / 2 mg	60 mg

2.2.3 Synthesis of ZnCdSSe quaternary alloyed quantum dots

Different amount of Zinc Stereate were used to introduce as zinc precursor into CdSSe tenary alloyed quantum dots' structure. Only difference of synthesizing ZnCdSSe QDs compared to CdSSe QDs was dissolving zinc stereate with cadmium myristate in 50 mL toluene which has already contained 1.50 g oleic acid (5.3 mmol) at 90 ^{0}C until clear solution obtained and this solution poured into main reaction balloon under nitrogen gas, where 60 mg thiourea (0,79 mmol) is dissolved in 40 mL distilled water and constant amount of 2 mL freshly prepared NaHSe solution was previously injected with glass syringe. Formed ZnCdSSe quaternary alloyed quantum dots were collected from toluene phase according to same time intervals explained in CdSSe QDs synthesis part and reaction is stopped after 24 hours. Toluene phase was separated from water phase by using separation funnel and after filtering and precipitating with methanol, quantum dots were obtained. Table 2.2 shows the used amounts of precursors to synthesize ZnCdSSe.

Table 2.2 : Used precursors' amount to synthesize ZnCdSSe.

Synthesis Code	CdMyristate	Zinc Stereate	NaHSe solution/ Se content	Thiourea
12_ME_ZnCdSSe	10 mg	0,19 g	2 mL / 2 mg	60 mg
6_ME_ZnCdSSe	0,1 g	0,1 g	2 mL / 2 mg	60 mg
11_ME_ZnCdSSe	0,15 g	50 mg	2 mL / 2 mg	60 mg

2.2.4 Synthesis of ZnCdSSeTe quinary alloyed quantum dots

Different amount of zinc stereate, cadmium myristate and 1,50 g oleic acid (5.3 mmol) were dissolved in 50 mL toluene under nitrogen gas at 90 ^{0}C and poured into 250 mL three-necked round bottom flask main reaction balloon, where 60 mg thiourea (0,79 mmol) and previously injected 2 mL freshly prepared NaHSe solution and altered amount of NaHTe solution found and forming quantum dots in toluene phase were collected within determined time intervals, which were given in CdSSe QDs synthesis part and reaction was stopped after 24 hours. Using separation funnel toluene phase separated from water phase and by filtering and adding methanol, quantum dots were obtained as precipitate. Table 2.3 shows the amounts of precursors used to synthesize ZnCdSSeTe.

Table 2.3 : Used amounts of precursors to synthesize ZnCdSSeTe.

Synthesis Code	Cd Myristate	Zinc Stereate	NaHSe solution/ Se content	NaHTe solution / Te content	Thiourea
19_ME_ZnCdSSeTe	10 mg	0,19 g	2 mL / 2 mg	2 mL / 5 mg	60 mg
18_ME_ZnCdSSeTe	50 mg	0,15 g	2 mL / 2 mg	2 mL / 5 mg	60 mg
17_ME_ZnCdSSeTe	0,1 g	0,1 g	2 mL / 2 mg	2 mL / 5mg	60 mg
25_ME_ZnCdSSeTe	10 mg	0,19 g	2 mL / 2 mg	4 mL / 10mg	60 mg
26_ME_ZnCdSSeTe	50 mg	0,15 g	2 mL / 2 mg	4 mL / 10 mg	60 mg
28_ME_ZnCdSSeTe	0,1 g	0,1 g	2 mL / 2 mg	4 mL / 10 mg	60 mg

3. RESULTS AND DISCUSSION

3.1 Optical and Structural Characterization

3.1.1 Fluorescence spectroscopy and UV-visible spectroscopy

Optical characterization is done by Fluorescence Spectroscopy with Varian Eclipse fluorescence spectrofluorometer and UV-Vis Spectroscopy with double beam Scinco Neosystometer 2000. For the Fluorescence measurements of quantum dots collected from toluene phase within determined time intervals were dissolved in toluene and 350-530 nm excitation wavelength range was used to obtain emission spectra. Maximum emission wavelengths of each quantum dots, determined from emission spectra, were used to obtain excitation spectrum. To obtain absorption spectra, collected quantum dots within determined time intervals were dissolved in hexane and every quantum dot colors were observed under UV-lamp with 366 nm UV-light irradiation [46,47].

3.1.2 X-ray diffraction spectrometry

Drop method was used for XRD measurements. According to this method, dichloromethane was chosen as volatile solvent, which enabled to collect and transfer quantum dots on to the sample holder without causing any change in the structure of quantum dots. After the evaporation of the solvent, measurements were done with RIGAKU SmartLab XRD spectrometer under 0.01 step (deg) with 4 seconds speed of duration time within the range 15 to 16 2-theta degree with Cu kα radiation at a wavelength of 1.5406 Å at 45 kV voltage [46].

3.2 For CdSSe Ternary Alloyed Quantum Dots

To be able to comprehend and compare the effect of composition on optical properties and structural properties of quaternary and quinary alloyed Cd-based quantum dots, CdSSe ternary alloyed quantum dots were synthesized first and used as original point of future modifications.

0.2 g cadmium myristate as cadmium precursor, 60 mg thiourea as sulfur precursor and 2 mL NaHSe solution as 2 mg selenium precursor contained CdSSe ternary alloyed quantum dots' growth were observed by using fluorescence spectroscopy and UV-Visible spectroscopy.

To obtain information about relation between reaction time and size of the quantum dots, approximately 2 mL of quantum dots were taken from the toluene phase of the reaction balloon during the synthesis at 1h and 3h. After 24 h, synthesis was stopped, and quantum dots were collected as precipitate by methanol addition to the separated and filtered toluene phase. The results showed that within the 1h and 3h, there is no significant differences in the size of the quantum dots, and they showed maximum emission approximately 410 nm. However, when the reaction proceeds to 24h, red shift in the wavelength observed and maximum emission wavelength found around 475 nm, which resulted blue colored emitting CdSSe ternary alloyed quantum dots. The similarity between the maximum emission wavelength of 1h and 3h proved growth of the quantum dots did not completely occur immediately after adding the precursor like hot-injection synthesis method and two- phase synthesis method served well to control size and monodispersity of the synthesized quantum dots by slow growth with the convenience of Caner Ünlü et al. 2013 findings [18]. Figure 3.1 shows emission spectra of 1h, 3h and 24h CdSSe ternary alloyed quantum dots excited with 350 nm excitation wavelength and Figure 3.2 shows the color of 24 h sample under 366 nm UV irradiation.

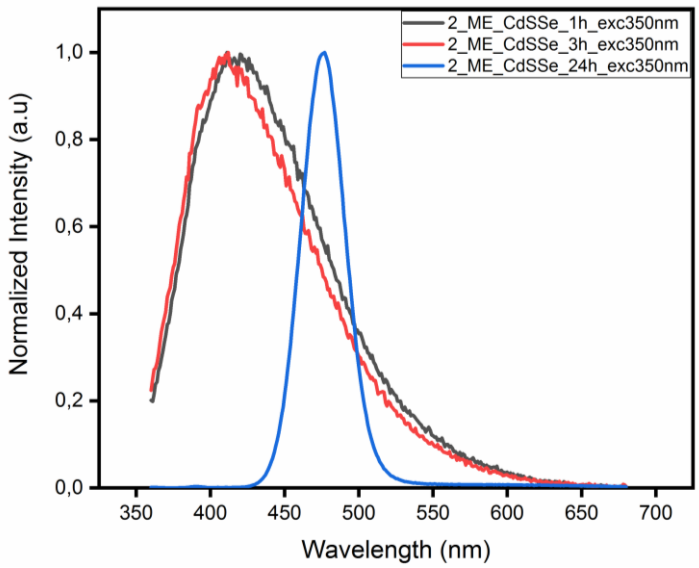

Figure 3.1 : Normalized emission spectra of 1h, 3h and 24h reaction time CdSSe ternary alloyed quantum dots.

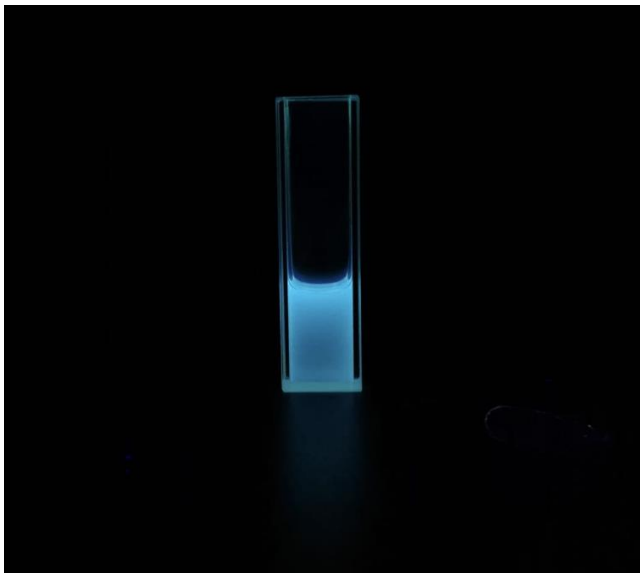

Figure 3.2 : 24 h CdSSe ternary alloyed quantum dots under UV lamp with 366 nm UV-irradiation.

Maximum emission wavelength 472 nm of 24 h CdSSe ternary alloyed quantum dots used to obtained excitation spectrum (Figure 3.3) to be able to compare excitation spectrum of future modifications done to form quaternaty and quinary alloyed quantum dots.

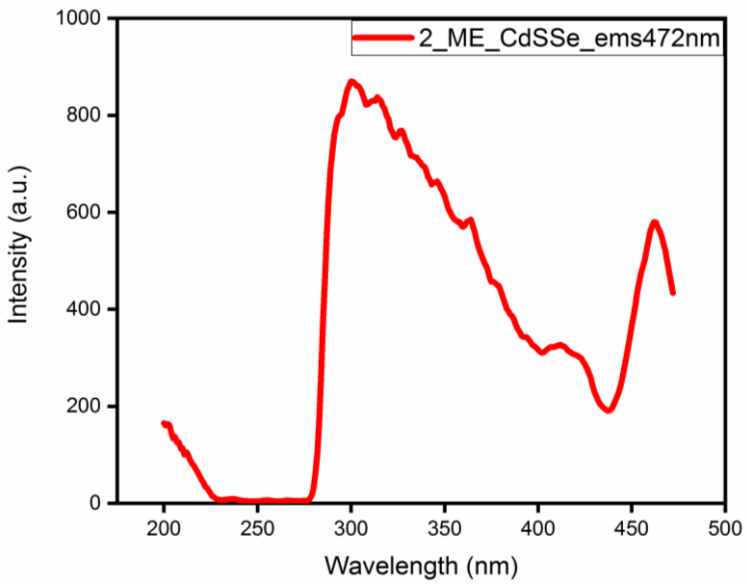

Figure 3.3 : Excitation spectrum of CdSSe ternary alloyed quantum dots under 472 nm emission wavelength.

Same 24h sample used for fluorescence spectroscopy measurement was used also for UV-Visible spectroscopy measurements and maximum absorbance found at approximately 460 nm (Figure 3.4). This maximum wavelength differences between the emission and absorption spectra can be explained by Stoke shift.

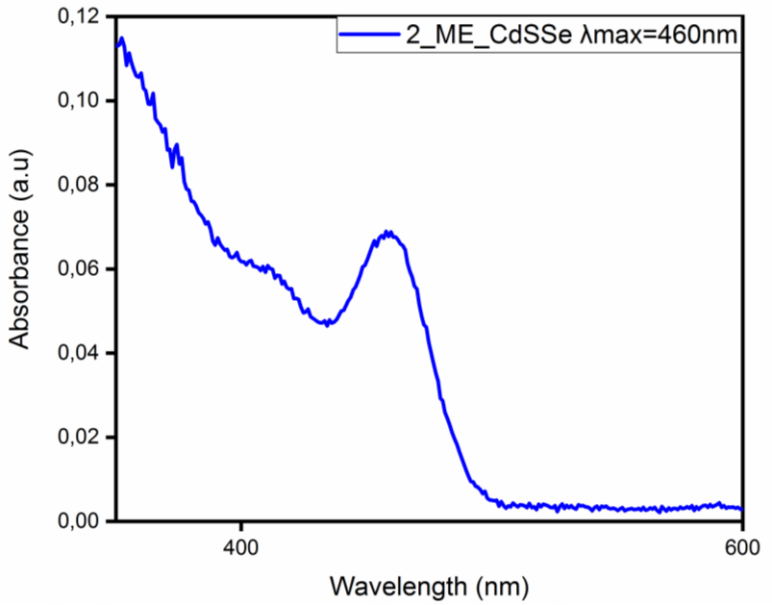

Figure 3.4 : UV spectrum of CdSSe ternary alloyed quantum dots with 24 h reaction time.

For the structural characterization, XRD measurements was done and unique quantum dots' broad peaks, which is caused by ultra-small size of the quantum dots, were obtained [18].

Three broad peaks observed at (111), (220) and (311) planes and when it is compared with the CdSe and CdSe diffraction angles at (111) plane, which are 25.53 and 26.506 respectively, it was found that CdSSe diffraction angle found between these angles 25.809 (Figure 3.5).

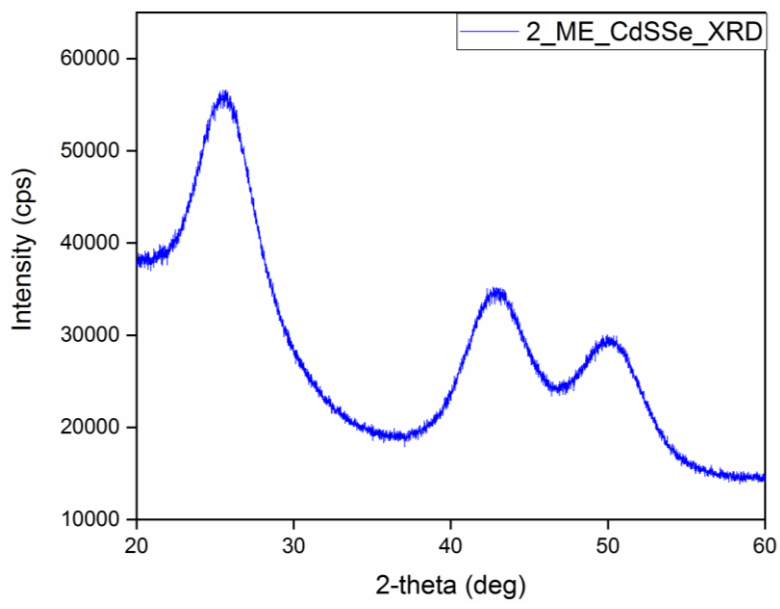

Figure 3.5 : XRD patterns of CdSSe ternary alloyed quantum dots.

3.3 For CdSSeTe Quaternary Alloyed Quantum Dots

While synthesizing CdSSeTe quaternary alloyed quantum dots, firstly it was investigated the effect of tellurium addition into the ternary alloyed CdSSe quantum dots' structure. Changing the amount of the added tellurium allowed to observe the tellurium effect on the aim of expanding CdSSe ternary alloyed quantum dots' absorption and controllable emission wavelength range.

Therefore, while synthesizing CdSSeTe quaternary alloyed quantum dots, amount of cadmium, selenium and sulfur precursor kept constant as found in previously synthesized CdSSe ternary alloyed quantum dots in order to be able to compare the results, which were respectively 0.2 g cadmium myristate, 2 mL NaHSe solution as 2 mg selenium and 60 mg thiourea as sulfur precursor.

Cadmium, selenium and sulfur amount kept constant while different amount of tellurium added to the reaction to form CdSSeTe quaternary alloyed quantum dots. It enabled to observe direct effect of tellurium on optical properties on CdSSeTe quaternary alloyed quantum dots while providing information the differences between the optical and structural properties with original CdSSe ternary alloyed quantum dots.

It was found that addition of the tellurium into the structure of ternary alloyed CdSSe quantum dot and increasing the amount of tellurium in the structure of quaternary alloyed CdSSeTe quantum dots caused red shift on fluorescence emission spectra (Figure 3.6) and on UV-Visible absorbance spectra by leading a decreasing on energy band gap of the CdSSe quantum dots (Figure 3.7, 3.8 and 3.9). These results are convenient since CdTe has lower energy band gap compared to CdSe and CdS. Therefore, tellurium addition in the structure lowers the energy gap between the valance and conduction band and the peaks shape became broader when the content of the tellurium increased in the structure, which is the feature of emission spectra of quantum dots contained tellurium in their structure.

2 mL and 4 mL NaHTe solution as 5 mg and 10 mg tellurium precursor respectively added to 0.2 g cadmium myristate as cadmium precursor, 60 mg thiourea as sulfur precursor and 2 mL NaHSe solution as 2 mg selenium precursor contained CdSSe ternary alloyed quantum dots. Fluorescence and UV spectroscopy measurements results showed that increasing the amount of the tellurium in the structure caused red shift as expected [14,48,49]. It proved the possibility to reach out of the limits of the

absorption and controllable emission wavelengths of the original ternary alloyed CdSSe quantum dots by modifying them with forming quaternary structure with the addition of tellurium.

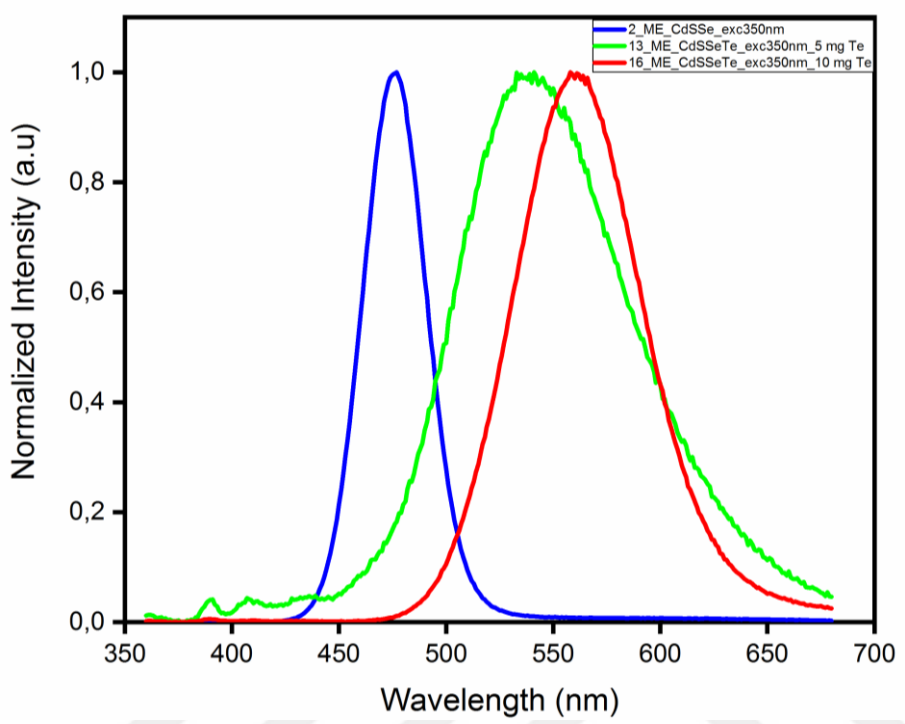

Figure 3.6 : Normalized emission spectra of CdSSe and CdSSeTe with 5 mg Te and CdSSeTe with 10 mg Te.

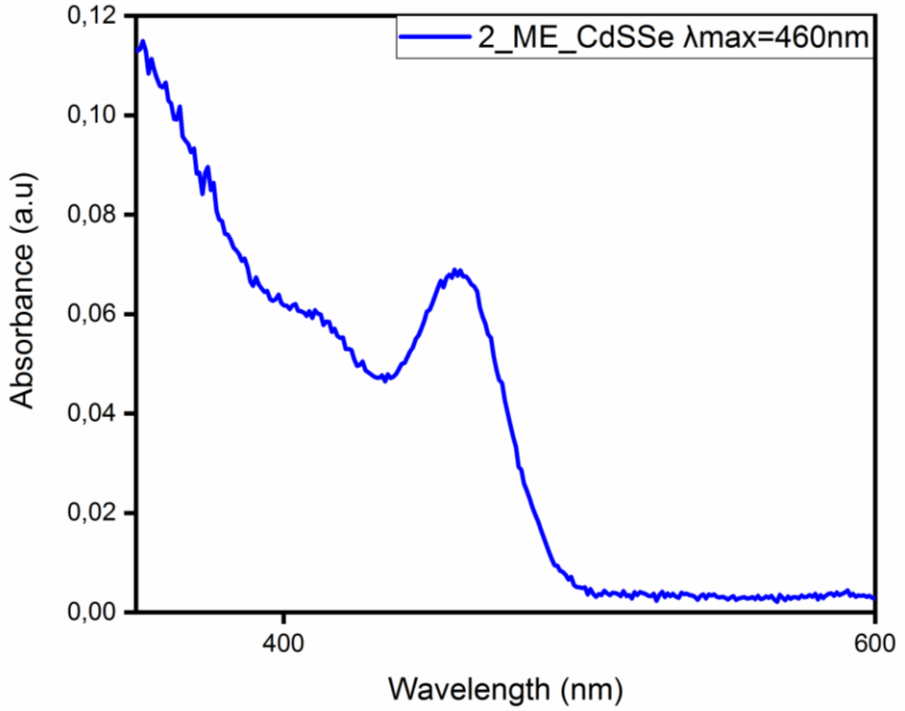

Figure 3.7 : Absorption spectrum of CdSSe ternary alloyed quantum dots.

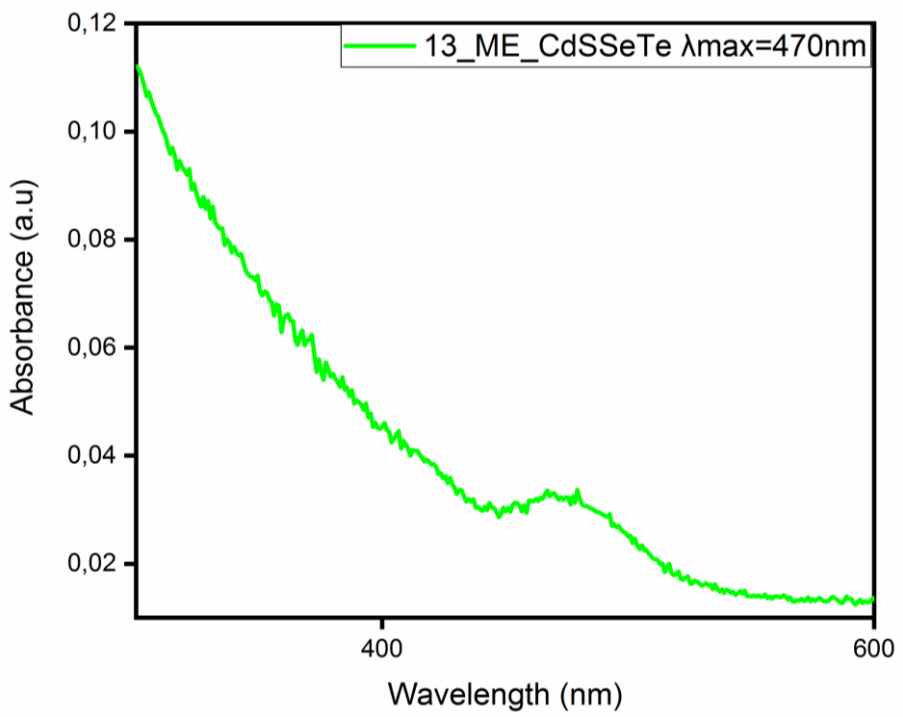

Figure 3.8 : Absorbtion spectrum of CdSSeTe quaternary alloyed quantum dot with 5 mg Te.

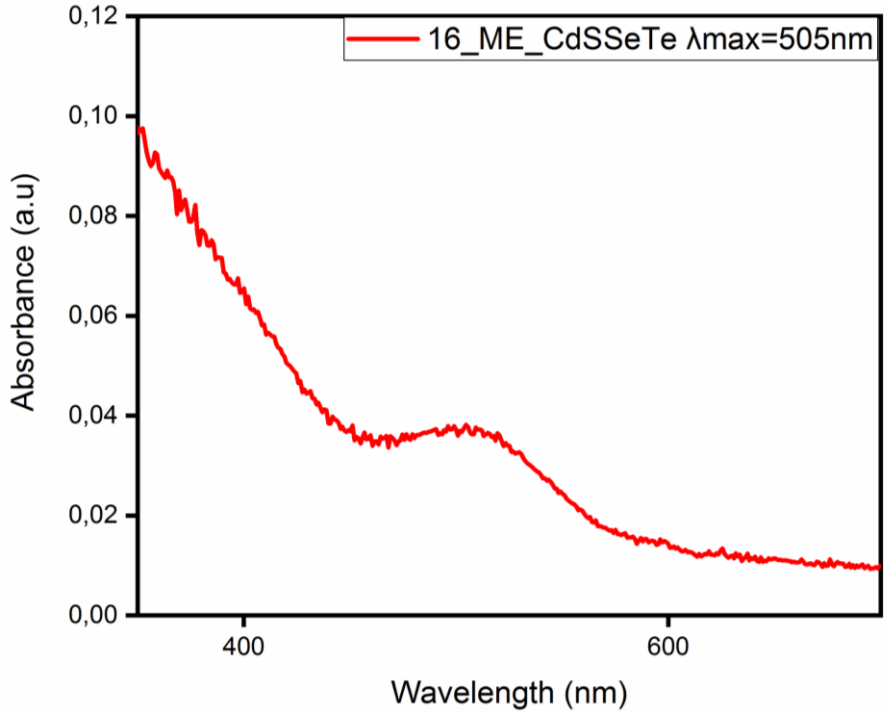

Figure 3.9 : Absorption spectrum of CdSSeTe quaternary alloyed quantum dot with 10 mg Te.

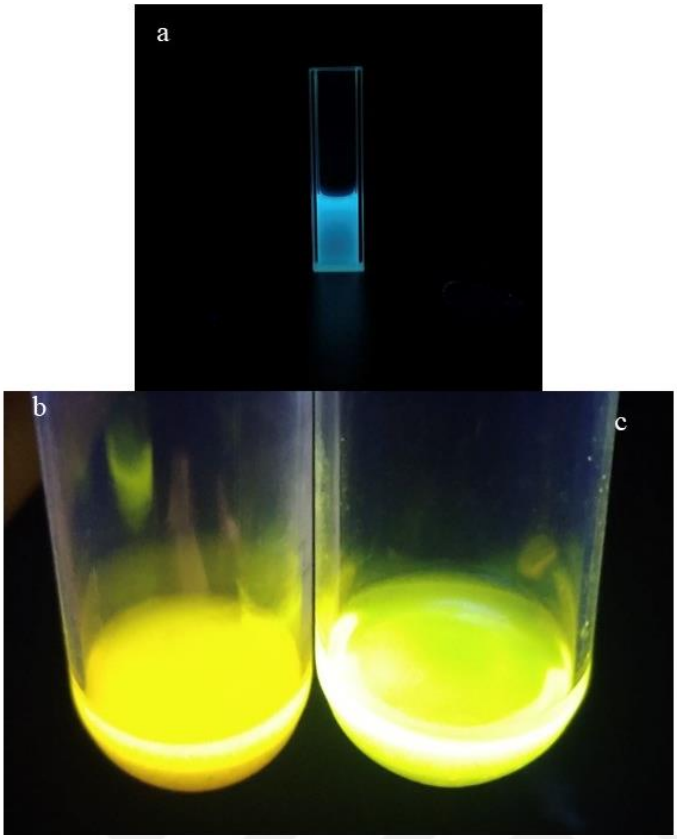

Figure 3.10 : a) CdSSe, b) CdSSeTe with 10 mg Te and c) CdSSeTe with 5 mg under 366 nm UV- irradiation.

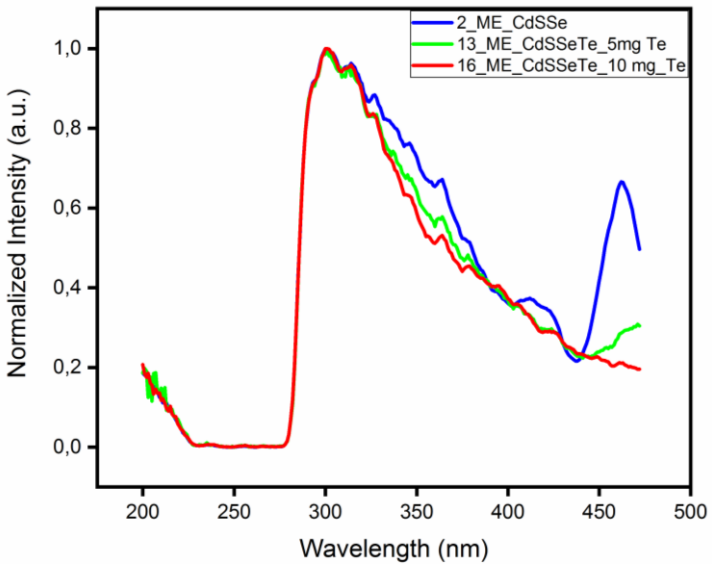

Figure 3.11 : CdSSe, CdSSeTe with 5 mg Te and CdSSeTe with 10 mg excitation spectra.

CdSSe ternary alloyed quantum dots, CdSSeTe with 5 mg Te and CdSSeTe with 10 mg Te excitation spectra obtain at 472 nm, 540 nm, and 561 nm emission wavelength respectively (Figure 3.11). Between 200 and 400 nm, spectra showed similarity, which corresponds absorption spectrum. However, after 400 nm represents band-edge

transition, CdSSeTe quaternary alloyed quantum dots showed different pattern with the CdSSe ternary alloyed quantum dots, since tellurium was added into the structure. This composition modification leaded the difference in the band-edge transition, which proved the addition of tellerium into the structure [50].

To understand the effect of the compositional modification on structure and crtystallinity,

XRD measurements were done (Figure 3.12) and it proved the addition of tellurium into the structure. Tellurium addition in the structure could be understood by diffraction angle shifting to the lower angle compared to the XRD pattern of CdSSe ternary alloyed quantum dots at plane (111), (220) and (311).

At (111) plane, for CdSSe ternary alloyed peaks found at 25.809 degree, which was between 25.53 degree and 26.51 degree respectively for CdSe JCPDS and CdS JCPDS.

However, at plane (111) CdSSeTe found lower degree compared to CdSSe ternary alloyed quantum dots which was seen at 25.46 degree for CdSSeTe with 5 mg Te and 24.47 degree for CdSSeTe with 10 mg Te. Lower shift increment with the addition of Tellurium into the structure was convenient, since CdTe JCPDS diffraction peak found at 23.84 2-theta degree [51].

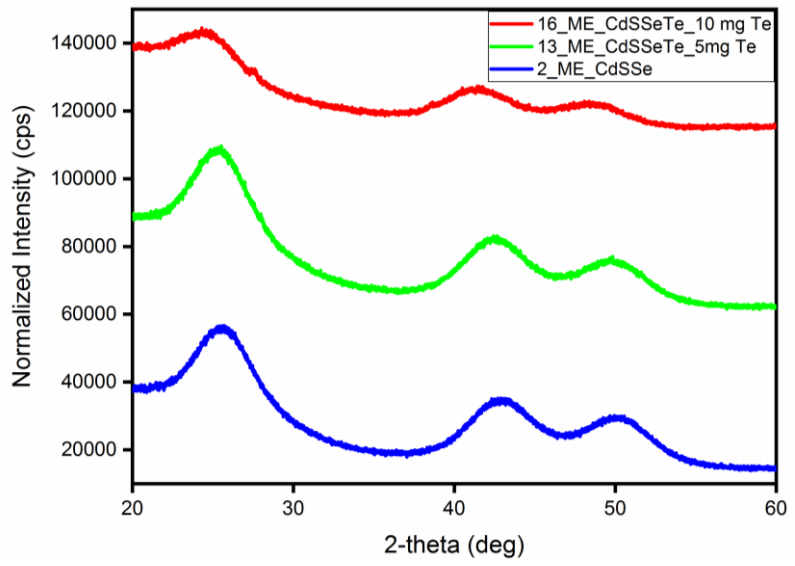

Figure 3.12 : CdSSe and CdSSeTe with 5 mg Te and CdSSeTe with 10 mg Te XRD patterns.

Secondly, to understand the importance of the Cadmium amount in the structure on optical properties, CdSSeTe quaternary alloyed quantum dots synthesized using 10 mg cadmium myristate, 2 mL NaHSe solution as 2 mg selenium 60 mg thiourea as sulfur

precursor and 2 mL NaHTe solution as 5 mg tellurium precursor and it was compared with 0.2 g cadmium precursor contained CdSSeTe quaternary alloyed quantum dots.

Although 0.2 g cadmium precursor contained CdSSeTe was very bright regardless of different ratio tellurium added in the structure. 10 mg cadmium precursor was not enough to obtain bright colored quantum dots under 366 nm UV-irradiation as seen in the Figure 3.13 and the fluorescence spectroscopy results showed that decreasing the amount of the cadmium caused blue shift under 350 nm excitation wavelength (Figure 3.14).

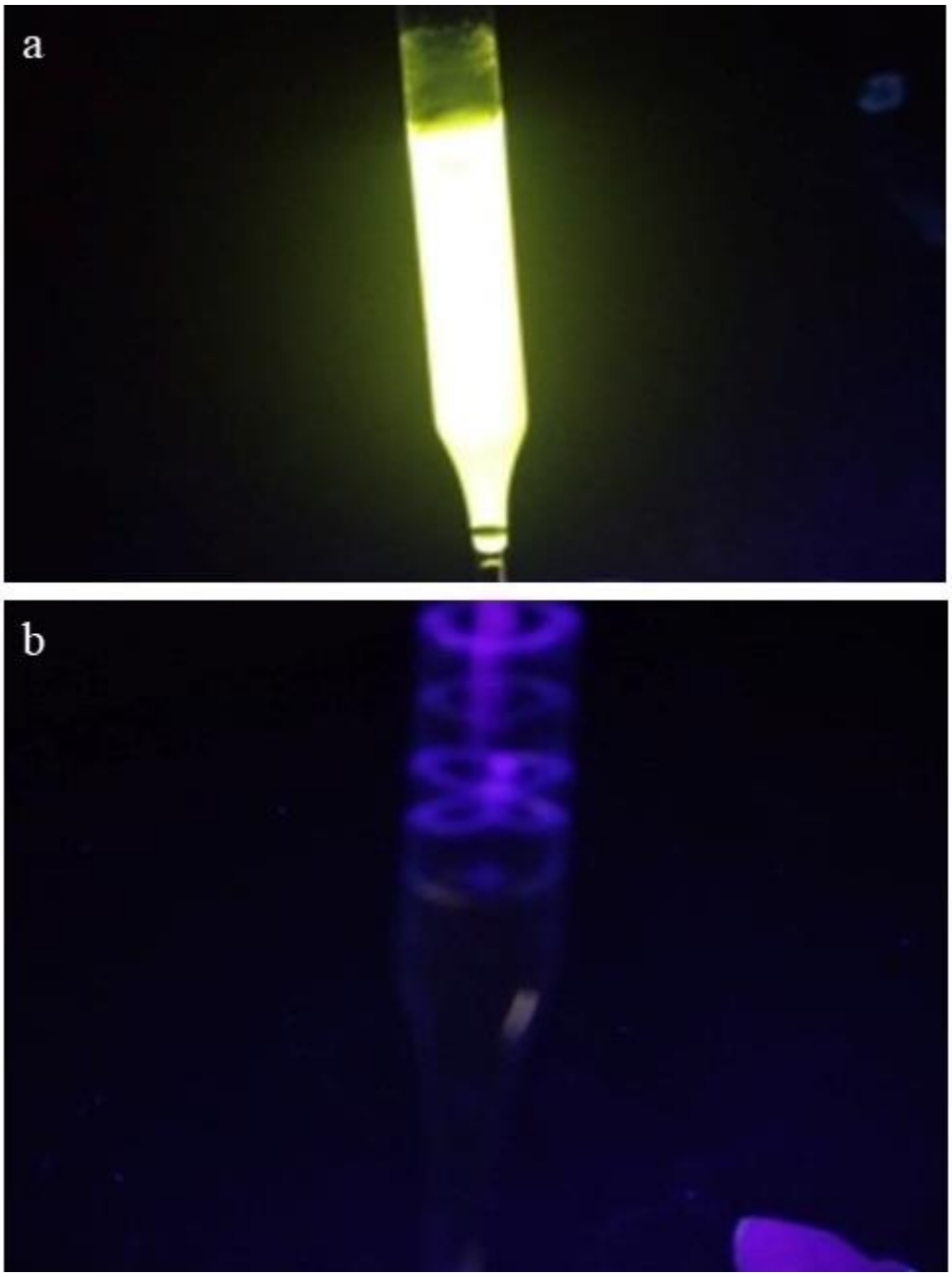

Figure 3.13 : a) CdSSeTe with 0.2 g Cadmium precursor and b) CdSSeTe with 10 mg Cadmium precursor under UV 366 nm UV-irradiation.

It was understood that cadmium amount is the key factor to obtain bright quantum dots and it enables to maintain advantageous optical properties of the original CdSSe ternary and CdSSeTe quaternary alloyed quantum dots.

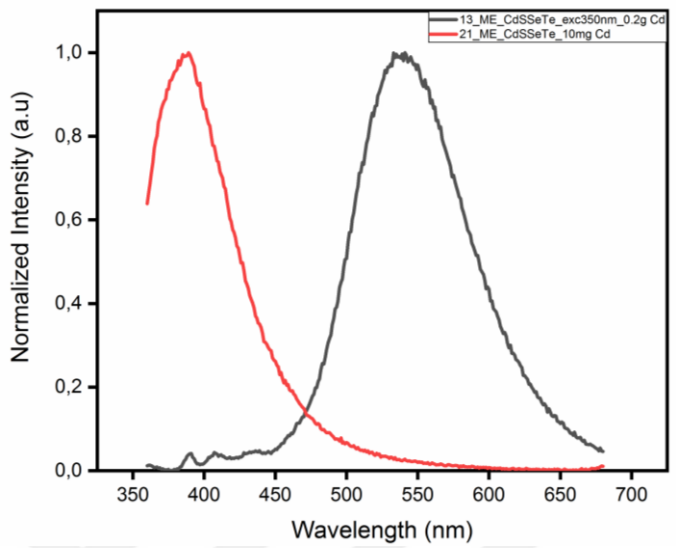

Figure 3.14 : Normalized emission spectra of CdSSeTe with 10 mg Cd and CdSSeTe with 0.2 g Cd.

3.4 For ZnCdSSe Quaternary Alloyed Quantum Dots

Addition of the zinc into the CdSSe ternary alloyed quantum dot structure investigated in order to understand the possibility of decreasing the amount of the cadmium found in the structure to prevent the negative effect of cadmium toxicity on application areas of the CdSSe ternary alloyed quantum dots.

Therefore, to understand the effect of zinc addition for lowering the amount of cadmium content originally found in CdSSe ternary alloyed quantum dots, amount of zinc and cadmium precursor altered while synthesizing ZnCdSSe quaternary alloyed quantum dots. Total amount of the cation precursors (cadmium myristate and zinc sterate as cadmium and zinc precursor) was kept constant as 0.2 g for all trials and 2mL NaHSe solution as 2 mg Selenium and 60 mg thiourea as sulfur precursor amount were used for all syntheses.

Pair of 0.1 g zinc stereate with 0.1 g cadmium myristate, 50 mg zinc stereate with 0.15 g cadmium myristate and 0.19 mg zinc stereate with 10 mg cadmium myristate contained ZnCdSSe quaternary alloyed quantum dots compared with the original CdSSe ternary alloyed quantum dots contained 0.2 g cadmium precursor in the structure.

Syntheses started by decreasing cadmium amount to 0.15 g with the addition of 50 mg zinc by forming quaternary alloyed ZnCdSSe quantum dots. It caused 5 nm blue shift in the emission spectrum compared to the CdSSe ternary alloyed quantum dots contained 0.2 g cadmium (Figure 3.15). It can be explained as ZnS and ZnSe have higher band gap compared to CdS and CdSe therefore, addition of zinc into the structure caused blue shift in emission spectrum. However, although violet color emission was seen under 366 nm UV-irradiation (Figure 3.18-b), UV results showed no significant absorbance (Figure 3.16) and for the XRD results, (111) (220) and (311) planes observed but (220) and (311) plane have low intensity peaks, therefore (111) plane was chosen to compare the results and shift could be seen at plane (111) more clearly and the diffraction angle found at 25.95 and it shifted to the higher degrees compared to (111) CdSSe ternary alloyed quantum dots' diffraction angle , which proved the zinc addition into the structure. Since ZnS JCPDS found at 28. 558, CdSe JCPDS found at 25.53 and CdS JCPDS found at 26.50, addition of zinc considered the reason of higher degree shift (Figure 3.17). To be able to see clear effect of zinc addition, to form ZnCdSSe quaternary alloyed quantum dots, amount of zinc increased to 0.1 g and cadmium amount lowered to 0.1 g, which is the half of the amount found in original CdSSe ternary alloyed structure. When emission spectrum compared, it was observed that maximum emission wavelength 26 nm shifted to the higher nanometers (Figure 3.15). This shift normally cannot be expected in binary and homogeneous alloyed systems since ZnS and ZnSe have higher energy band compared to CdS and CdSe. Therefore, it can be considered as modification with zinc addition caused blue shift in binary and homogeneous alloyed systems. However, in this case it was observed oppositely. In Deng et al., 2009 study, synthesized uniform alloyed ZnCdSSe quaternary alloyed quantum dots' maximum emission wavelength shifted to the higher nanometers when CdSe amount increased in the structure compared to ZnS amount since CdSe has lower energy band gap compared to ZnS [52]. Tuning the band gap can be more predictable in homogeneous alloyed system since there is no optical bowing seen in this type of quantum dots. However, gradient alloyed systems have nonhomogeneous structure in their inner core and outer part. This non-homogeneity leads gradient alloyed quantum dots contain components having different energy within the structure and it results distorted energy bands instead of having discrete form of energy bands. Therefore, optical bowing can be occurred by providing non-linear relation of optical properties against the composition content [53]. In Bailey &

Nie, 2003 study, this phenomenon observed within CdSSeTe quaternary alloyed quantum dots, they found that tellurium content increment caused red shift at some extent. However, when Te content exceeded to %60, emission wavelength starts to shift lower naometers and they called this non-linear relation unique, and it was achieved since the structure belong to the gradient alloyed system [14].

Same red shift proved with absorption spectrum (Figure 3.19) and under 366 nm UV-irradiation, change in the color to green with modification of adding 0.1 g Zn and lowering the Cd amount to 0.1 g was seen. (Figure 3.18- c).

When XRD results of CdSSe with 0.2 g Cd and ZnCdSSe with 0.1 g Zn and 0.1 g Cd precursors compared, it was seen same diffraction angles peak at plane (111), (220) and (311) as broad peaks caused by ultra-small size of the quantum dots. The main difference in the diffraction angle was that shift to the higher diffraction angles for ZnCdSSe quaternary alloyed quantum dots in every plane. When (111) plane examined, it was seen that diffraction peak of CdSSe ternary alloyed quantum dots was found at 25.809 2-theta degree, which was convenient with CdS JCPDS found at 26.506 and CdSe JCPDS found at 25.53 degree. However, ZnCdSSe quaternary alloyed diffraction peak was seen at 26.296 degree. This proved zinc addition in the structure since originally ZnS JCPDS diffraction angle found at 28.558 2-theta degree, therefore after addition of Zinc into the structure caused shift toward higher degree (Figure 3.20). As a result, cadmium amount can be lowered by half of its amount found in the correspondent CdSSe ternary alloyed system and also it enabled to expand absorption and controllable emission wavelength at the same time.

To investigate the possibility of lowering cadmium more than 0.1 g, synthesis was done with 0.19 g Zinc and 10 mg Cadmium precursor addition. Although under 366 nm UV radiation light blue colored emission was seen (Figure 3.18- d), emission spectrum showed distorted peak and absorption spectra showed no significant absorption (Figure 3.15 and Figure 3.16). XRD patterns proved that the structure was not ZnCdSSe quaternary alloyed quantum dots since there was only one diffraction peak at plane (111). (Figure 3.17).

In addition, excitation spectra of CdSSe ternary alloyed quantum dots, ZnCdSSe with 50 mg, 0.1 g and 0.19 g Zn results were obtained with 472 nm, 471 nm, 503 nm, and 422 nm emission wavelength respectively (Figure 3.21). CdSSe and ZnCdSSe 50 mg,

0.1 g Zn showed for the representation of absorption spectrum between 200 – 400 nm wavelength similarity However, after 400 nm, which represents band-edge transition, ZnCdSSe with 0.19 g Zn quaternary alloyed quantum dots showed different pattern with the CdSSe and the rest of ZnSSe with 50 mg and 0.1 g Zn quantum dots. It proved that 0.19 g zinc addition cannot be achieved with preserving the quantum dots optical and structural properties. However, 0.1 g zinc addition could be done by lowering the cadmium amount found in the parent ternary alloyed system while expanding its controllable emission limits.

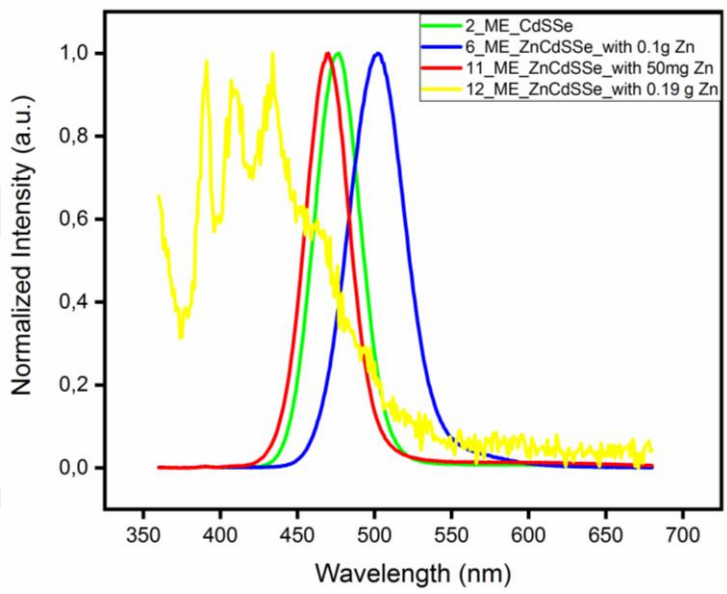

Figure 3.15 : Normalized emission spectra of CdSSe, ZnCdSSe with 0.1 g Zn, 50 mg Zn and 0.19 mg Zn.

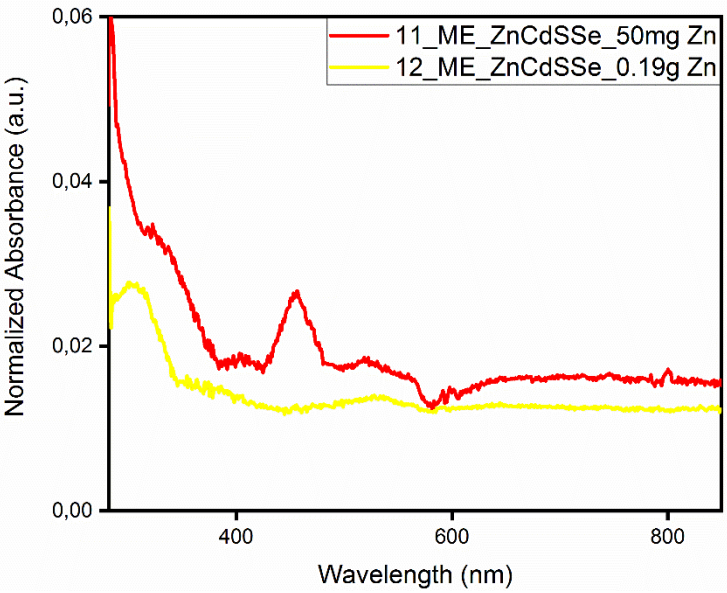

Figure 3.16 : Normalized absorption spectra of ZnCdSSe with 0.19 g and 50 mg Zn.

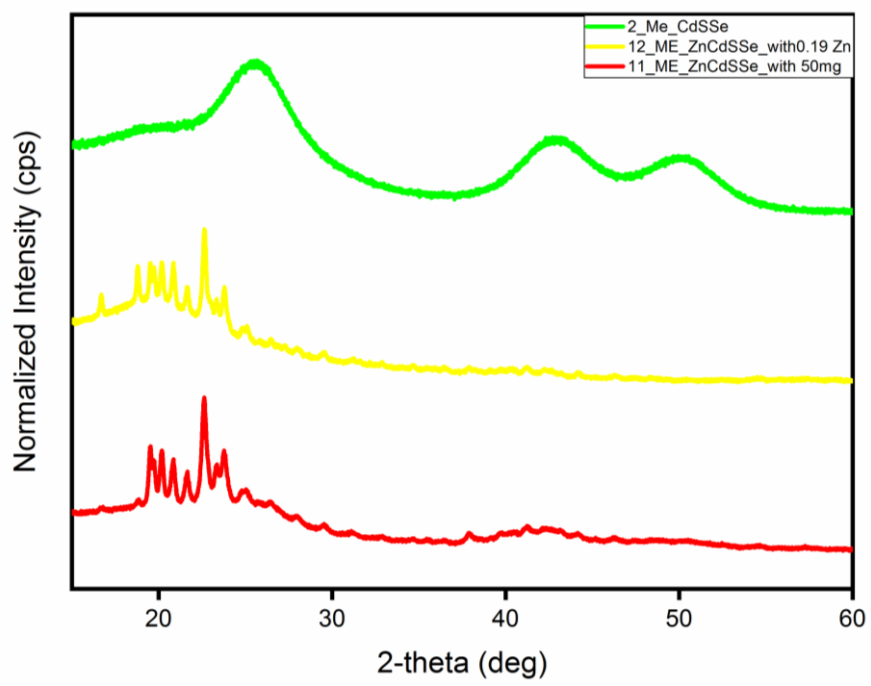

Figure 3.17 : Normalized XRD spectra of CdSSe and ZnCdSSe with 0.19 g and 50 mg Zn.

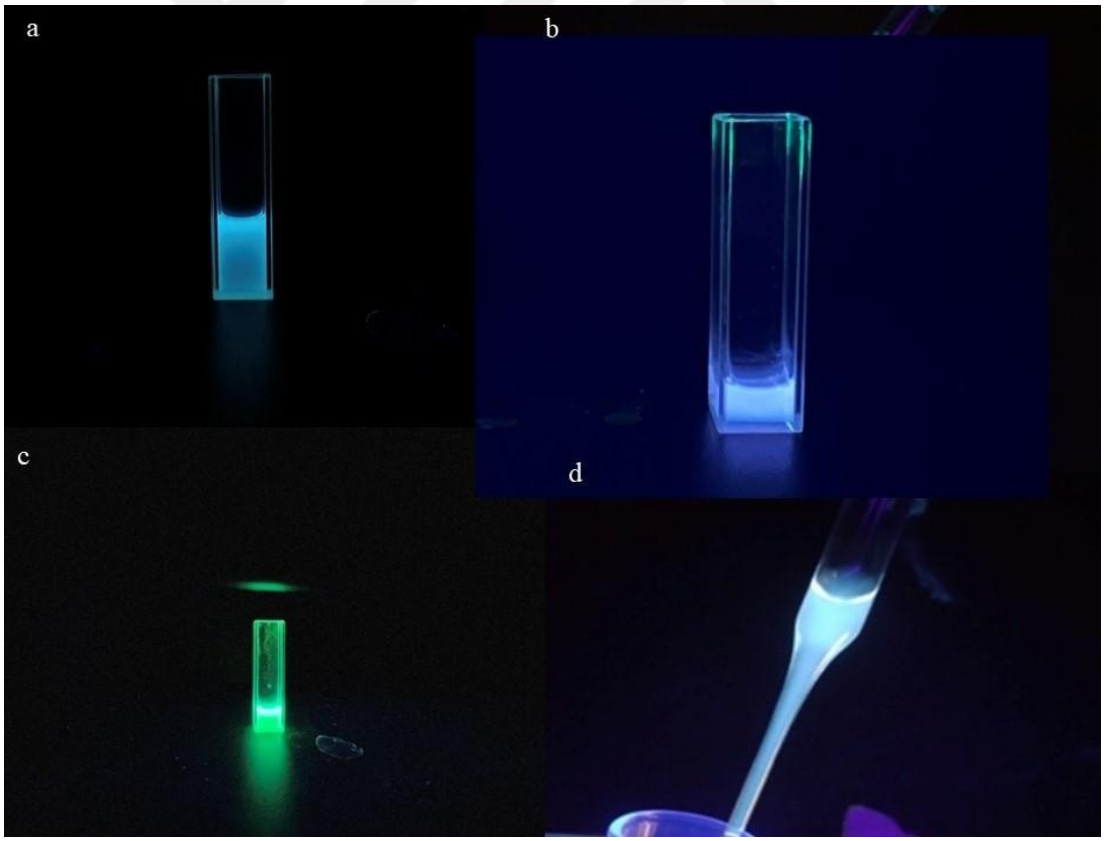

Figure 3.18 : Emission colors of a) CdSSe, b) ZnCdSSe with 50 mg Zn, c) ZnCdSSe with 0.1 g Zn and d) ZnCdSSe with 0.19 g Zn under 366nm UV-irradiation.

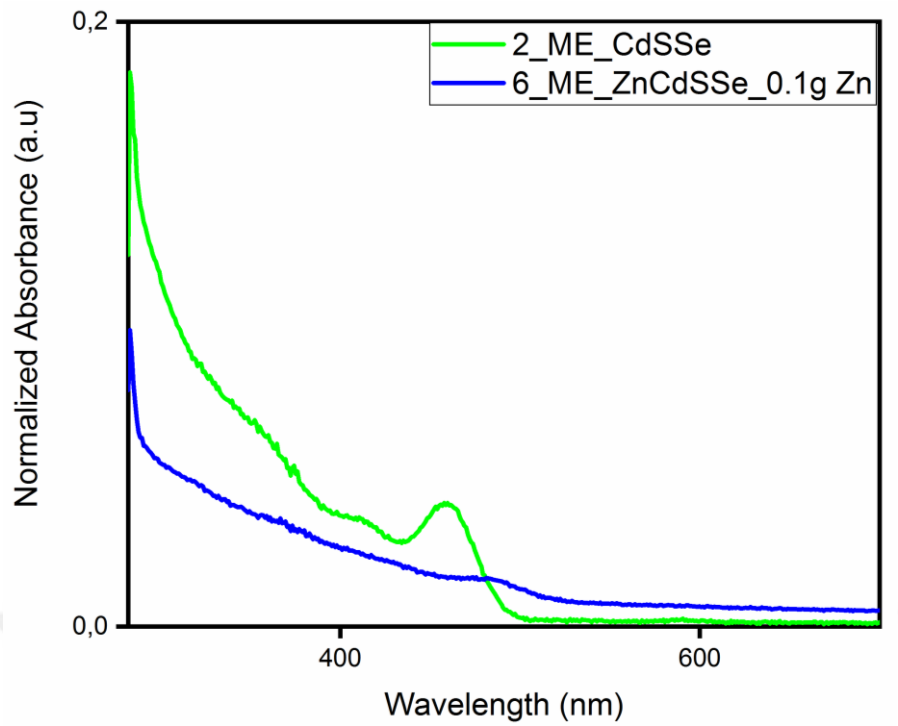

Figure 3.19 : Normalized Absorbance spectra of CdSSe and ZnCdSSe with 0.1 g Zn.

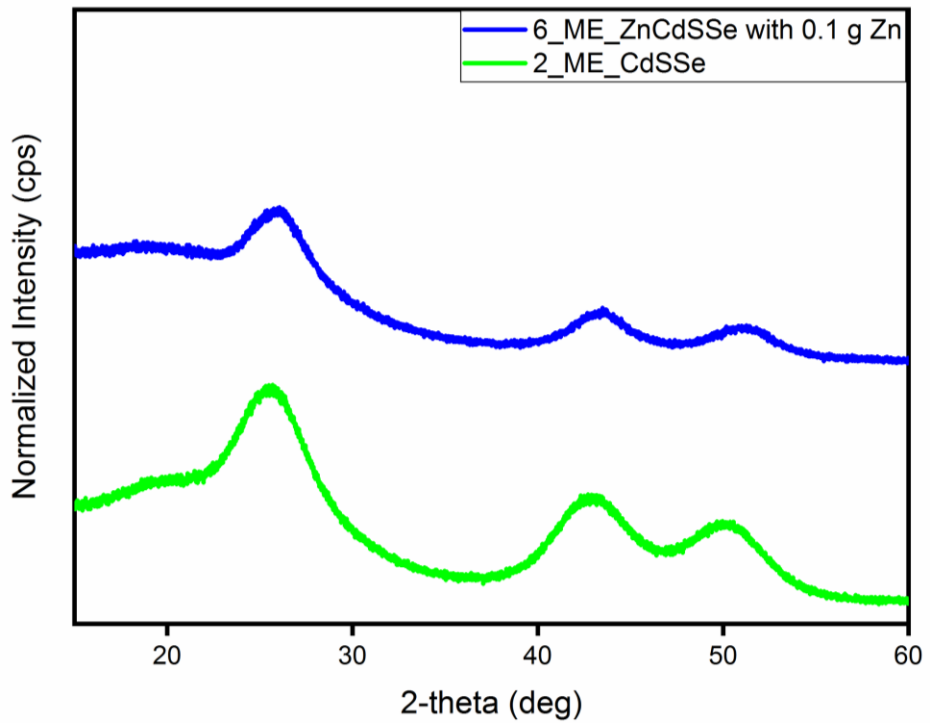

Figure 3.20 : Normalized XRD spectra of CdSSe and ZnCdSSe with 0.1 g Zn.

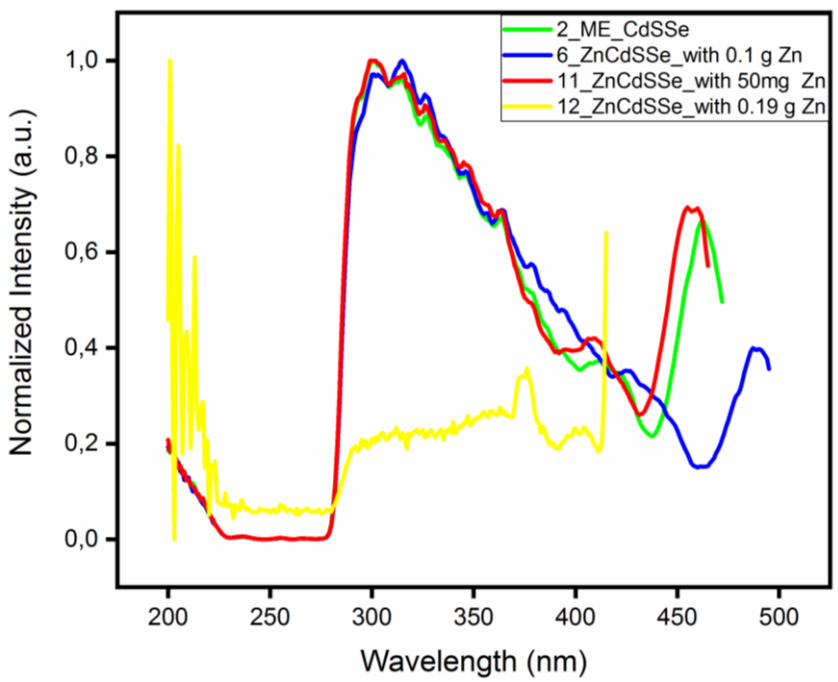

Figure 3.21 : CdSSe, ZnCdSSe with 50 mg, 0.1 g and 0.19 g Zn excitation spectra.

For further investigation for XPS measurements was done for ZnCdSSe with 0.1 g Zn and 0.1 g Cd, and it is found that ZnCdSSe ratio was 0.15:0.35:0.35:0.15 (Figure 3.22). Cadmium content was decreased by %30 with zinc addition and (HR) XPS analysis showed 2 broad peaks for Zn 2p, Cd 3d, S 2p and Se 3d, which proved alloyed structure since each atom made different types of bonds with more than two different atoms. (Figure 3.23).

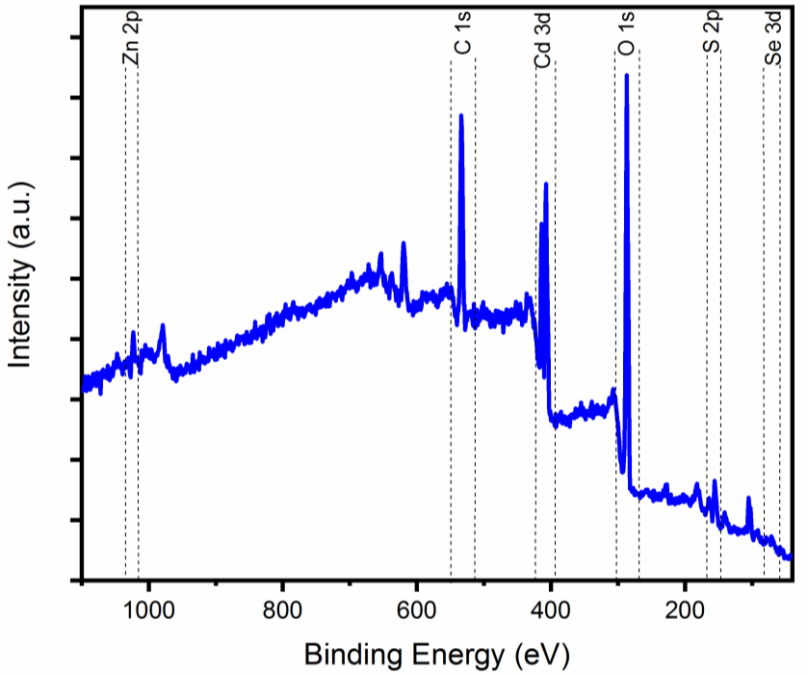

Figure 3.22 : XPS measurements for ZnCdSSe with 0.1 g Zn and 0.1 g Cd [17].

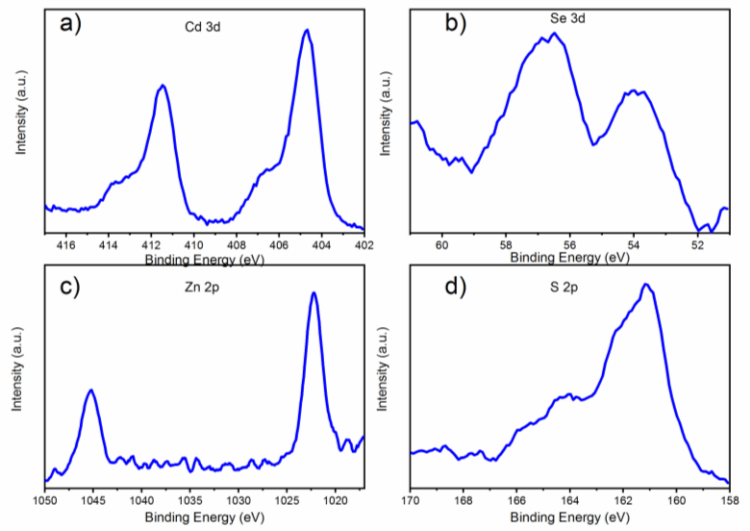

Figure 3.23 : HR XPS spectrum of a) Cd b) Se, c) Zn and d) S elements in ZnCdSSe with 0.1 g Zn and 0.1 g Cd [17].

Photostability of ZnCdSSe with 0.1 g Zn and 0.1 g Cd also investigated, precipitated ZnCdSSe florescence spectra obtained by dissolving in toluene on 1 day and 15 day and FL intensity of the 1 day and 15 day measurement of both solutions did not show significant differences, therefore it was understood that solid form of ZnCdSSe was phaotostable at ambient conditions (Figure 3.24- a). Then ZnCdSSe precipitation was dissolved in toluene and same solution was measured at 1, 4, 7, 10 and 15 days after. Results showed that FL intensity of 1 day dissolved ZnCdSSe quantum dots was decreased %30 after 15 days, which showed that quantum dots became unstable in solution compared to the solid form (Figure 3.24-b) It could be explained as solvent lead defects on the surface of quantum dots and resulted to form trap states, which caused intensity decrease. To investigate the effect of continuous laser exposure to ZnCdSSe quantum dots, they dissolved in toluene and during 30 min, solution was exposed to laser source. Results showed that ZnCdSSe quantum dots are stable against laser source exposure (Figure 3.24 -c).

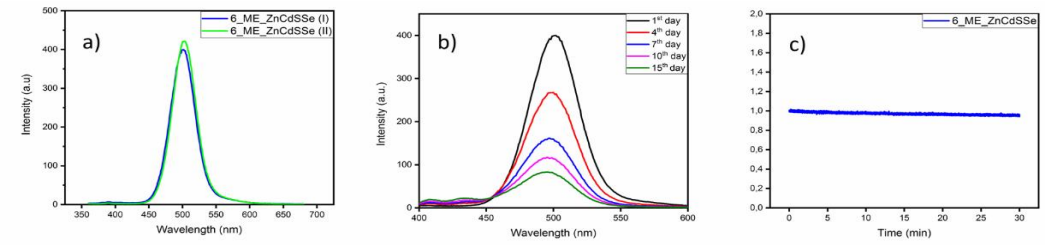

Figure 3.24 : Photostability of ZnCdSSe with 0.1 g Zn and 0.1 g Cd a) QD dissolved in toluene at 1 day and 15 day b) QD dissolved in toluene and measurements was done at 1,4,7,10,15 days for the same solution c) QD dissolved in toluene and exposed to laser during 3 [17].

3.5 For ZnCdSSeTe Quinary Alloyed Quantum Dots

After quaternary alloyed ZnCdSSe (0.1 g Zn and 0.1 g Cd) results showed the possibility of lowering cadmium amount found in the original ternary alloyed CdSSe structure with the addition of zinc while expanding of controllable emission wavelength by providing green colored quantum dots thanks to gradient alloyed structure, addition of both Tellurium and zinc into the ternary alloyed structure by transforming them quinary alloyed quantum dots was investigated in order to understand the possibility of decreasing cadmium amount in the structure more than it was found with the modification of forming quaternary alloyed quantum dots. Tellurium addition was planned along with the addition of zinc in order to achieve lowering cadmium amount and expanding controllable emission wavelength range at the same time.

Therefore, syntheses started altering zinc precursor amount while added amount of tellurium kept constant as 5 mg (2mL NaHTe solution). Total of the cation precursors (zinc stereate and cadmium myristate) was 0.2 g and pair of 0.1 g zinc stereate with 0.1 g cadmium myristate, 0.15 g zinc stereate with 50 mg cadmium myristate and 0.19 mg zinc stereate with 10 mg cadmium myristate were used to obtained quinary alloyed ZnCdSSeTe quantum dots.

Another series of syntheses were completed to understand the tellurium effect on optical properties of the modified quinary alloyed quantum dots. In these series, tellurium content was increased to 10 mg and same pair of cation precursors used to obtained comparable results with the 5 mg contained quinary alloyed quantum dots.

When 5 mg Te contained quinary alloyed quantum dots' emission spectrum compared with ternary alloyed CdSSe emission spectrum (Figure 3.25), 0.1 g Zn with 0.1 g cadmium and 0.19 g Zn with 10 mg Cd peaks were obtained approximately at the same maximum wavelength with CdSSe ternary alloyed quantum dots. However, 0.15 g Zn with 50 mg Cd provided two different peaks, which lead to conclude this ratio provide non-uniform structure of formed quantum dots, which means there are two different energy states providing different emission wavelength. Therefore, it was seen that monodisperse gradient alloyed quantum dots could not be obtained with this ratio. Under 366 nm UV-radiation quinary alloyed ZnCdSSeTe quantum dots for all pairs emitted light blue and blue color as CdSSe ternary alloyed quantum dots (Figure 3.26).

Excitation spectra of quinary alloyed quantum dots for pair of 0.1 g zinc stereate with 0.1 g cadmium myristate at 496nm, 0.15 g zinc stereate with 50 mg cadmium myristate at 473 nm and 0.19 mg zinc stereate with 10 mg cadmium myristate at 468 nm showed similar results at the both absorption and band-edge transition wavelength range with CdSSe ternary alloyed quantum dots (Figure 3.27). However, only 0.1 g Zn, 0.1 g Cd with 5 mg Te quinary alloyed ratio showed absorbance in UV spectra (Figure 3.28) and all of the ratios did not show any specific peaks at diffraction angles correspondent with the quantum dots presence (Figure 3.30). Therefore, it proved with these ratios, quinary alloyed quantum dots could not be obtained.

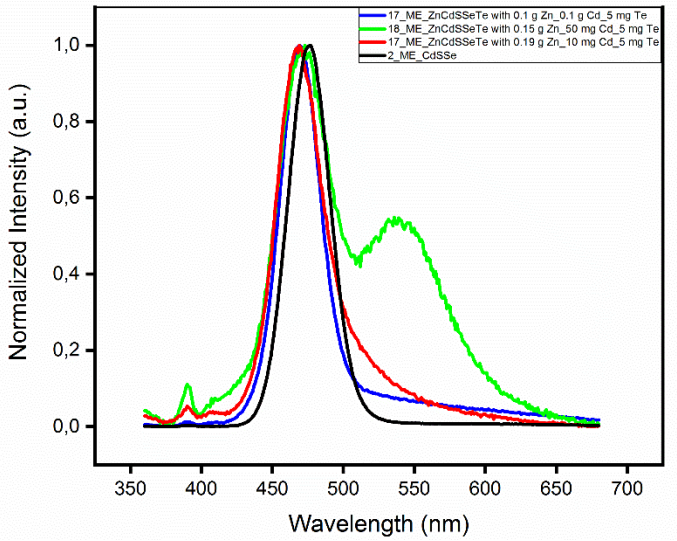

Figure 3.25 : Normalized emission spectra of CdSSe, ZnCdSSeTe with 0.1 g Zn, 0.15 g Zn and 0.19 mg Zn.

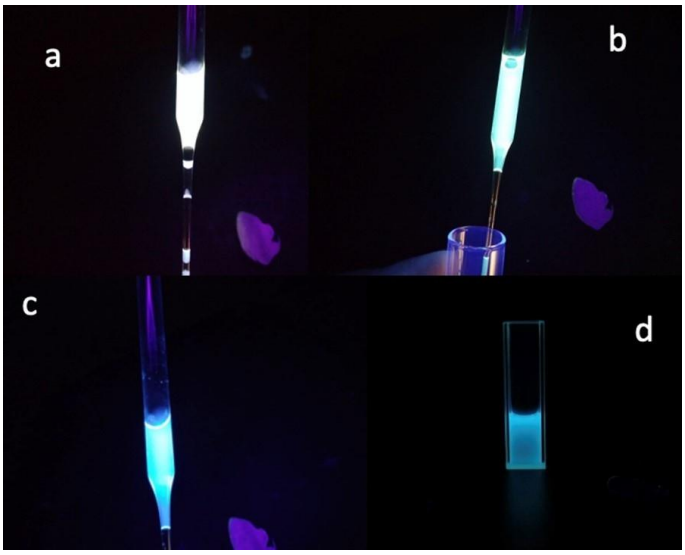

Figure 3.26 : Emission colors of a) ZnCdSSeTe with 0.1 g Zn, 0.1 g Cd and 5mg Te b) ZnCdSSeTe with 0.15 g Zn, 50 mg Cd and 5 mg Te c) ZnCdSSeTe with 0.19 g Zn, 10 mg Cd and 5 mg Te d) CdSSe with 0.2 g Zn under 366nm UV-irradiation.

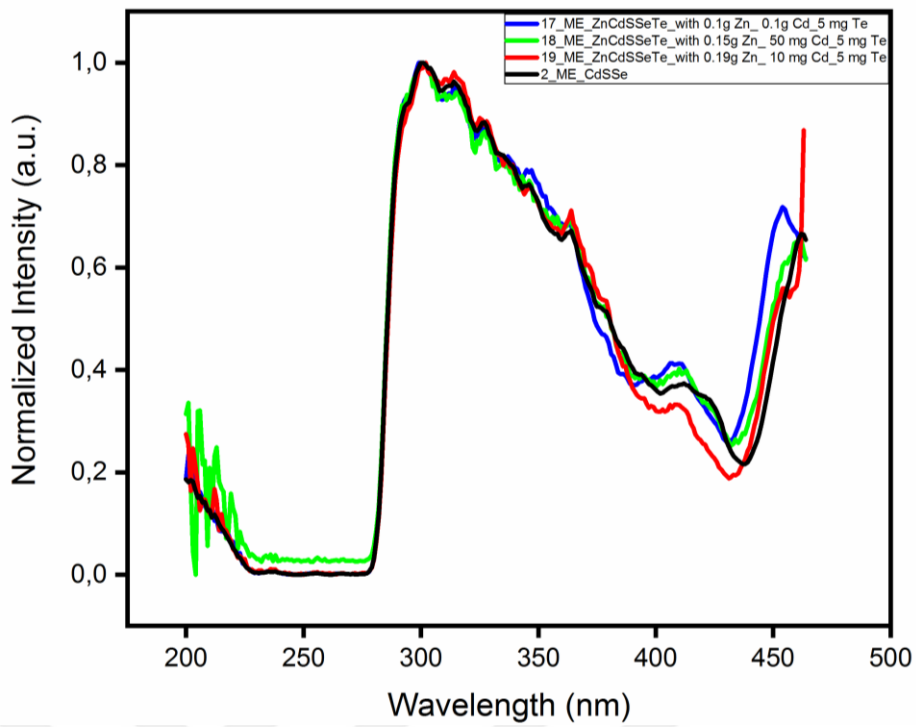

Figure 3.27 : Normalized excitation spectra of CdSSe, ZnCdSSeTe with 0.1 g Zn, 0.15 g Zn and 0.19 mg Zn.

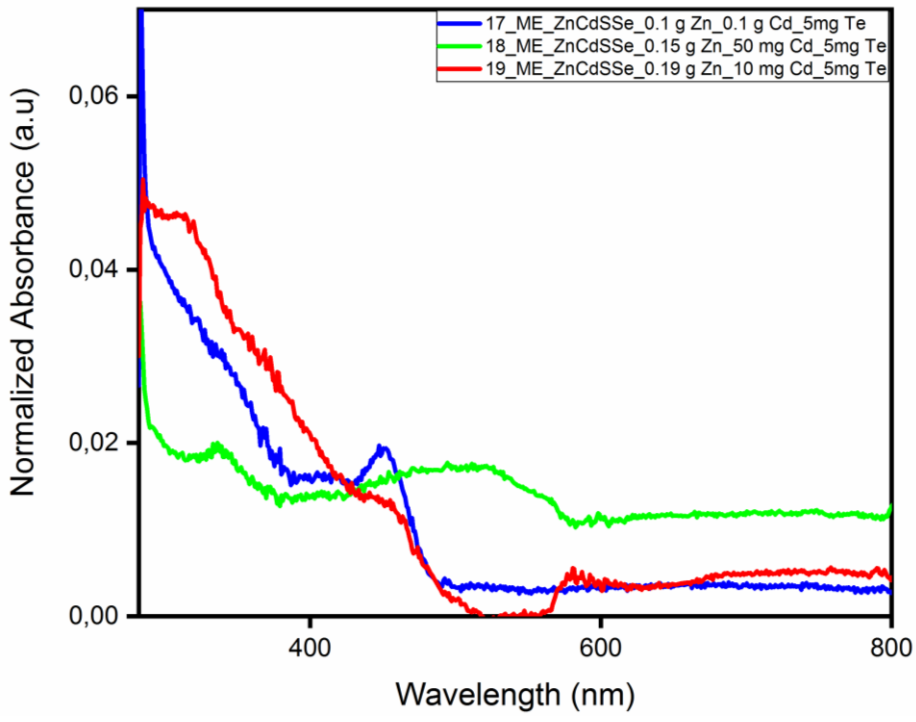

Figure 3.28 : Normalized absorption spectra of CdSSe, ZnCdSSeTe with 0.1 g Zn, 0.15 g Zn and 0.19 mg Zn.

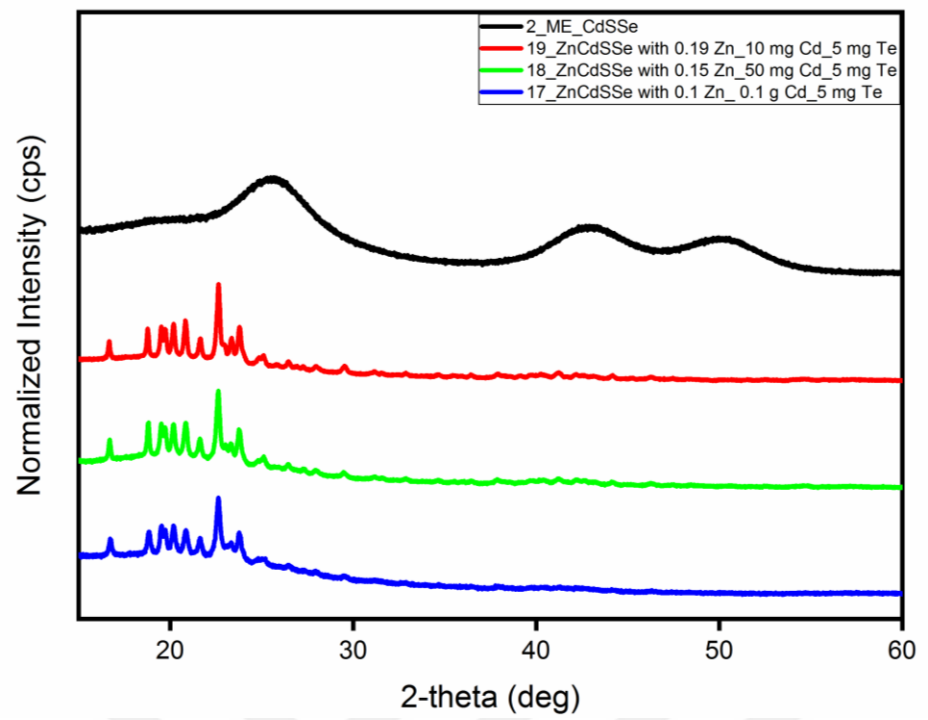

Figure 3.29 : Normalized XRD spectra of CdSSe, ZnCdSSeTe with 0.1 g Zn, 0.15 g Zn and 0.19 mg Zn.

To understand the effect of tellurium, same pair of cations used for syntheses, but in this case Te amount increased to 10 mg (4 mL NaHTe solution).

When emission spectrum observed only 0.1 g Zn, 0.1 g Cd and 10 mg Te contained quinary alloyed quantum dots showed significant peaks at 551 nm with clear red shift compared to original CdSSe ternary alloyed quantum dots (Figure 3.30). Although under 366 nm UV-irradiation, yellow colored was seen (Figure 3.31), in UV absorption spectra, it was not observed any absorption peaks (Figure 3.34) and for XRD results, there is no peaks at diffraction angles which proves the presence of the quantum dots (Figure 3.32). These results were also supported by excitation spectrum and between 200-400 nm wavelength, which represents absorption and after 400 nm wavelength for band-edge transition, there was not found any similar results of quantum dots presence (Figure 3.33).

As a result, quinary alloyed quantum dots could not be achieved by two phase synthesized method.

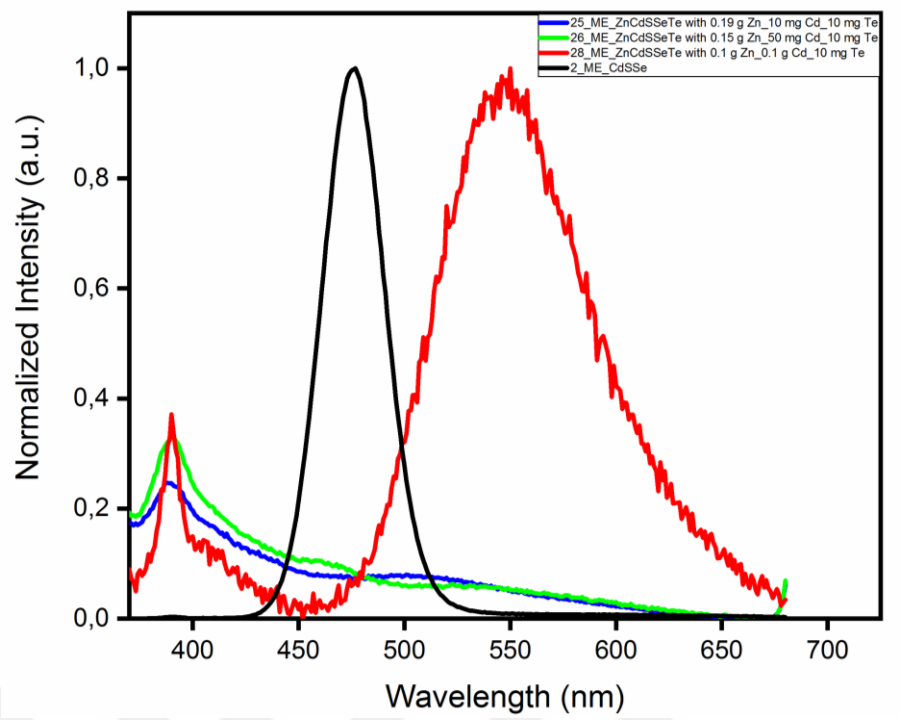

Figure 3.30 : Normalized emission spectra of CdSSe, ZnCdSSeTe with 0.1 g Zn, 0.15 g Zn and 0.19 mg Zn.

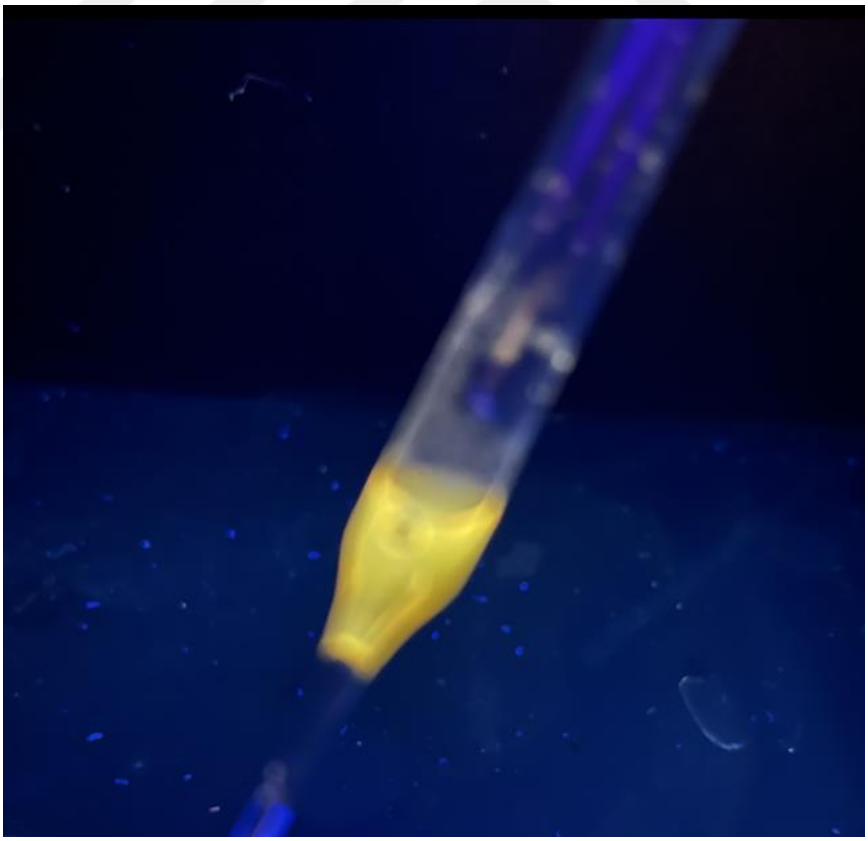

Figure 3.31 : Emission color of ZnCdSSeTe with 0.1 g, 0.1 g Cd and 10 mg Te.

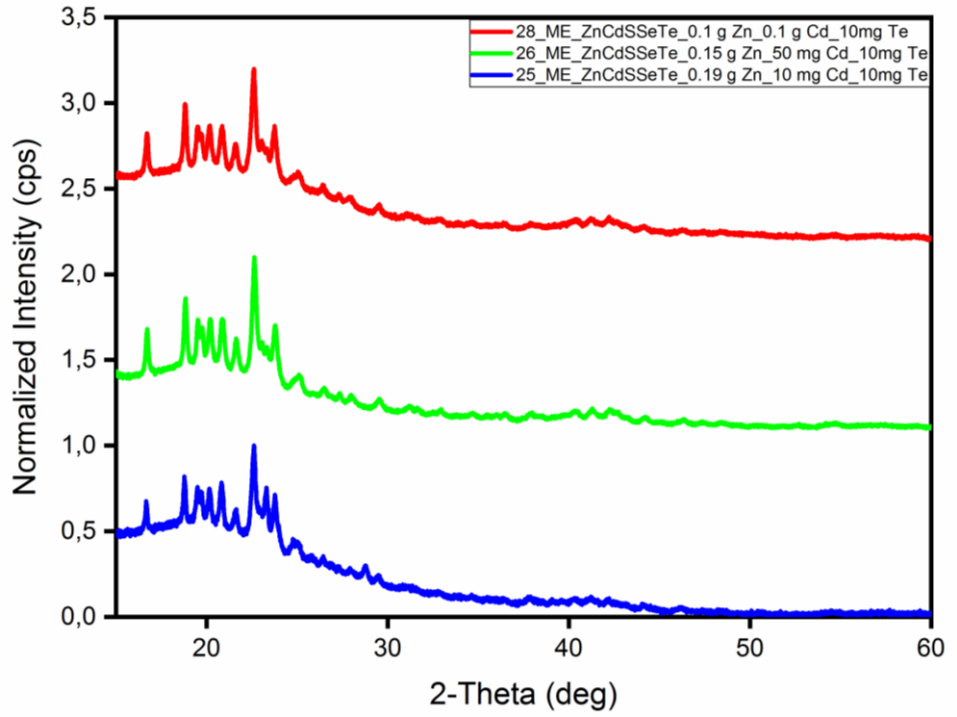

Figure 3.32 : Normalized XRD spectra of CdSSe, ZnCdSSeTe with 0.1 g Zn, 0.15 g Zn and 0.19 mg Zn with 10mg Te.

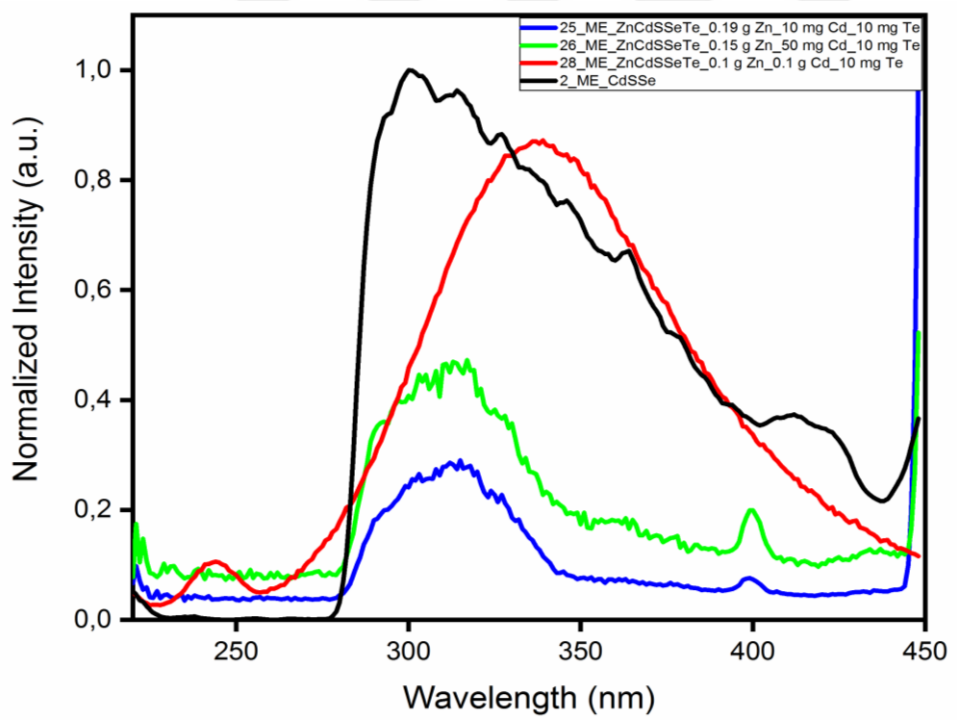

Figure 3.33 : Normalized excitation spectra of CdSSe, ZnCdSSeTe with 0.1 g Zn, 0.15 g Zn and 0.19 mg Zn.

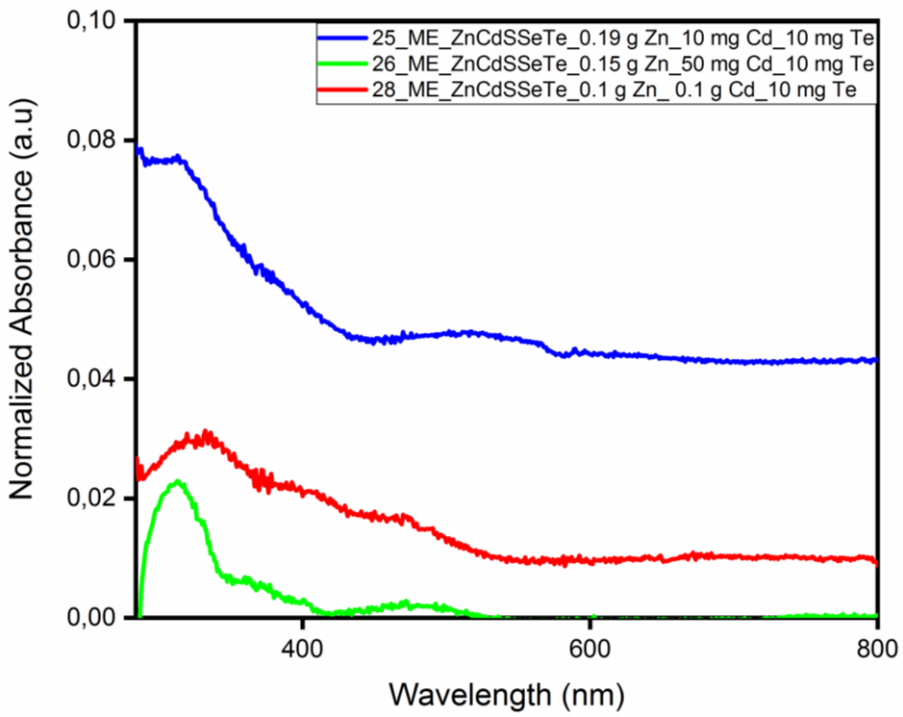

Figure 3.34 : Normalized absorption spectra of CdSSe, ZnCdSSeTe with 0.1 g Zn, 0.15 g Zn and 0.19 mg Zn.

4. CONCLUSION

In this thesis, the aim of increasing application area of CdSSe ternary alloyed quantum dots by expanding controllable emission wavelength range and lowering the cadmium amount in the structure could be reached by forming CdSSeTe and ZnCdSSe. It was obtained that increasing the Tellurium amount in the structure caused red shift and yellow color emitted CdSSeTe quaternary alloyed quantum dots obtained with 5 mg and 10 mg tellurium addition. With the addition of zinc, cadmium amount could be lowered half of the amount found in the original CdSSe ternary alloyed quantum dots and at the same time zinc addition resulted to be obtained green color emitted ZnCdSSe quaternary alloyed quantum dots, which showed it was also achieved to expand controllable emission wavelength range of the CdSSe ternary alloyed quantum dots.

However, synthesizing ZnCdSSeTe quinary alloyed quantum dots via two-phase synthesis method could not be achieved. From the optical and structural results, there was not seen any sign, which showed the presence of the quinary alloyed quantum dot could not be obtained.

REFERENCES

[1] **Maxwell, T., Nogueira Campos, M. G., Smith, S., Doomra, M., Thwin, Z., & Santra, S. (2020).** Quantum Dots. Nanoparticles for Biomedical Applications, 243–265. https://doi.org/10.1016/b978-0-12-816662-8.00015-1

[2] **Cotta, M. A. (2020).** Quantum dots and their applications: What lies ahead? ACS Applied Nano Materials, 3(6), 4920–4924. https://doi.org/10.1021/acsanm.0c01386

[3] **Mohamed, W. A., Abd El-Gawad, H., Mekkey, S., Galal, H., Handal, H., Mousa, H., & Labib, A. (2021).** Quantum Dots synthetization and future Prospect Applications. Nanotechnology Reviews, 10(1), 1926–1940. https://doi.org/10.1515/ntrev-2021-0118.

[4] **Nozik, A. J., Beard, M. C., Luther, J. M., Law, M., Ellingson, R. J., & Johnson, J. C. (2010).** Semiconductor quantum dots and quantum dot arrays and applications of multiple exciton generation to third-generation photovoltaic solar cells. Chemical Reviews, 110(11), 6873–6890. https://doi.org/10.1021/cr900289f

[5] **Hakimian, F., Ghourchian, H., Hashemi, A. sadat, Arastoo, M. R., & Behnam Rad, M. (2018).** Ultrasensitive optical biosensor for detection of mirna-155 using positively charged au nanoparticles. Scientific Reports, 8(1). https://doi.org/10.1038/s41598-018-20229-z

[6] **Mansur, A. A., Mansur, H. S., Carvalho, S. M., Lobato, Z. I., Leite, M. de, & Mansur, L. L. (2018).** Fluorescent zns quantum dots–phosphoethanolamine nanoconjugates for bioimaging live cells in cancer research. ACS Omega, 3(11), 15679–15691. https://doi.org/10.1021/acsomega.8b02098

[7] **Li, R., Tang, L., Zhao, Q., Teng, K. S., & Lau, S. P. (2020).** Facile synthesis of ZnS quantum dots at room temperature for ultra-violet photodetector applications. Chemical Physics Letters, 742, 137127. https://doi.org/10.1016/j.cplett.2020.137127

[8] **Pidluzhna, A., Ivaniuk, K., Stakhira, P., Hotra, Z., Chapran, M., Ulanski, J., Tynkevych, O., Khalavka, Y., Baryshnikov, G. V., Minaev, B. F., & Ågren, H. (2019).** Multi-channel electroluminescence of CdTe/cds core-shell quantum dots implemented into a QLED device. Dyes and Pigments, 162, 647–653. https://doi.org/10.1016/j.dyepig.2018.10.074

[9] **Ruzycka-Ayoush, M., Kowalik, P., Kowalczyk, A., Bujak, P., Nowicka, A. M., Wojewodzka, M., Kruszewski, M., & Grudzinski, I. P. (2021).** Quantum dots as targeted doxorubicin drug delivery nanosystems in human lung cancer cells. Cancer Nanotechnology, 12(1). https://doi.org/10.1186/s12645-021-00077-9

[10] **Brus, L. E. (1984).** Electron–electron and electron- hole interactions in small semiconductor crystallites: The size dependence of the lowest excited electronic state. The Journal of Chemical Physics, 80(9), 4403–4409. https://doi.org/10.1063/1.447218

[11] **Pleskova, S., Mikheeva, E., & Gornostaeva, E. (2018).** Using of quantum dots in biology and medicine. Advances in Experimental Medicine and Biology, 323–334. https://doi.org/10.1007/978-3-319-72041-8_19

[12] **Bera, D., Qian, L., Tseng, T.-K., & Holloway, P. H. (2010).** Quantum dots and their multimodal applications: A Review. Materials, 3(4), 2260–2345. https://doi.org/10.3390/ma3042260

[13] **Alami, A. H., & Faraj, M. (2022).** Quantum Dots: Types and characteristics. Encyclopedia of Smart Materials, 183–191.https://doi.org/10.1016/b978-0-12-815732-9.00018-8

[14] **Bailey, R. E., & Nie, S. (2003).** Alloyed Semiconductor Quantum Dots: tuning the optical properties without changing the particle size. Journal of the American Chemical Society, 125(23), 7100–7106.https://doi.org/10.1021/ja035000o

[15] **de Mello Donegá, C., Liljeroth, P., & Vanmaekelbergh, D. (2005).** Physicochemical evaluation of the hot-injection method, a synthesis route for monodisperse nanocrystals. Small, 1(12), 1152–1162. https://doi.org/10.1002/smll.200500239

[16] **Murray, C. B., Norris, D. J., & Bawendi, M. G. (1993).** Synthesis and characterization of nearly monodisperse cde (e = sulfur, selenium, tellurium) semiconductor nanocrystallites. Journal of the American Chemical Society, 115(19), 8706–8715. https://doi.org/10.1021/ja00072a025

[17] **Erkan, M., Ük, N., Nar, I., & Ünlü, C. (2023).** Adapting two-phase synthesis method to develop cadmium poor Quaternary ZnCd-chalcogenide quantum dots. Optical Materials, 138, 113713. https://doi.org/10.1016/j.optmat.2023.113713

[18] **Ünlü, C., Tosun, G. Ü., Sevim, S., & Özçelik, S. (2013**). Developing a facile method for highly luminescent colloidal cdsxse1−x ternary nanoalloys. Journal of Materials Chemistry C, 1(17), 3026. https://doi.org/10.1039/c3tc00077j

[19] **Chen, N., He, Y., Su, Y., Li, X., Huang, Q., Wang, H., Zhang, X., Tai, R., & Fan, C. (2012).** The cytotoxicity of cadmium-based Quantum Dots. Biomaterials, 33(5), 1238–1244. https://doi.org/10.1016/j.biomaterials.2011.10.070

[20] **Genchi, G., Sinicropi, M. S., Lauria, G., Carocci, A., & Catalano, A. (2020).** The effects of cadmium toxicity. International Journal of Environmental Research and Public Health, 17(11), 3782. https://doi.org/10.3390/ijerph17113782

[21] **Ikeri, H. I., Onyia, A. I., ., ., & Vwavware, O. J. (2019).** The dependence of confinement energy on the size of Quantum Dots. International Journal of Scientific Research in Physics and Applied Sciences, 7(2), 27–30. https://doi.org/10.26438/ijsrpas/v7i2.2730

[22] **URL-1** <https://uwaterloo.ca/chem13-news-magazine/november-2017/feature/quantum-dots-harnessing-nanoscopic-rainbow> Retrieved July 16, 2022

[23] **Takagahara, T. (2002).** EXCITONIC structures and optical properties of Quantum Dots. Semiconductor Quantum Dots, 59–114. https://doi.org/10.1007/978-3-662-05001-9_2

[24] **Smith, A. M., & Nie, S. (2009).** Semiconductor nanocrystals: Structure, properties, and band Gap Engineering. Accounts of Chemical Research, 43(2), 190–200. https://doi.org/10.1021/ar9001069

[25] **J. Sinclair and Dr. Dagotto (2009),** "An Introduction to Quantum Dots: Confinement, Synthesis, Artificial Atoms and Applications," Solid State II Lecture Notes, University of Tennessee, Knoxville.

[26] **Reimann, S. M., & Manninen, M. (2002).** Electronic structure of quantum dots. Reviews of Modern Physics, 74(4), 1283–1342. https://doi.org/10.1103/revmodphys.74.1283

[27] **Deerinck, T. J. (2008).** The application of fluorescent quantum dots to confocal, multiphoton, and electron microscopic imaging. Toxicologic Pathology, 36(1), 112–116. https://doi.org/10.1177/0192623307310950

[28] **har, M. J. (2017).** A review on Aptamer-conjugated quantum dot nanosystems for Cancer Imaging and Theranostic. Journal of Nanomedicine Research, 5(3). https://doi.org/10.15406/jnmr.2017.05.00117

[29] **Giansante, C., & Infante, I. (2017).** Surface traps in colloidal quantum dots: A combined experimental and Theoretical Perspective. The Journal of Physical Chemistry Letters, 8(20), 5209–5215. https://doi.org/10.1021/acs.jpclett.7b02193

[30] **Sadjadi, S. (2021).** The utility of carbon dots for photocatalysis. Emerging Carbon Materials for Catalysis, 123–160. https://doi.org/10.1016/b978-0-12-817561-3.00004-4

[31] **Bae, W. K., Joo, J., Padilha, L. A., Won, J., Lee, D. C., Lin, Q., Koh, W.-kyu, Luo, H., Klimov, V. I., & Pietryga, J. M. (2012).** Highly effective surface passivation of PbSe quantum dots through reaction with molecular chlorine. Journal of the American Chemical Society, 134(49), 20160–20168. https://doi.org/10.1021/ja309783v

[32] **Lei, D., Shen, Y. T., Feng, Y. Y., & Feng, W. (2012).** Recent progress in the fields of tuning the band gap of Quantum Dots. Science China Technological Sciences, 55(4), 903–912. https://doi.org/10.1007/s11431-011-4717-1

[33] **Loukanov, A. R., Dushkin, C. D., Papazova, K. I., Kirov, A. V., Abrashev, M. V., & Adachi, E. (2004).** Photoluminescence depending on the ZnS shell thickness of cds/zns core-shell semiconductor nanoparticles. Colloids and Surfaces A: Physicochemical and Engineering Aspects, 245(1-3), 9–14. https://doi.org/10.1016/j.colsurfa.2004.06.016

[34] **Dorfs, D., Hickey, S., & Eychmüller, A. (2011).** Type-I and type-ii core-shell quantum dots: Synthesis and characterization. Nanotechnologies for the Life Sciences. https://doi.org/10.1002/9783527610419.ntls0199

[35] **Vasudevan, D., Gaddam, R. R., Trinchi, A., & Cole, I. (2015).** Core–Shell Quantum Dots: Properties and applications. Journal of Alloys and Compounds, 636, 395–404. https://doi.org/10.1016/j.jallcom.2015.02.102

[36] **Petryayeva, E., Algar, W. R., & Medintz, I. L. (2013).** Quantum dots in bioanalysis: A review of applications across various platforms for fluorescence spectroscopy and imaging. Applied Spectroscopy, 67(3), 215–252. https://doi.org/10.1366/12-06948

[37] **Li, H., Wang, C., Peng, Z., & Fu, X. (2015).** A review on the synthesis methods of cdses-based nanostructures. Journal of Nanomaterials, 2015, 1–16. https://doi.org/10.1155/2015/519385

[38] **Zhang, W., Zhang, H., Feng, Y., & Zhong, X. (2012).** Scalable single-step noninjection synthesis of high-quality core/shell quantum dots with emission tunable from violet to near infrared. ACS Nano, 6(12), 11066–11073. https://doi.org/10.1021/nn304765k

[39] **Gurusinghe, N. P., Hewa-Kasakarage, N. N., & Zamkov, M. (2008).** Composition-tunable properties of cdsxte1−x alloy nanocrystals. The Journal of Physical Chemistry C, 112(33), 12795–12800. https://doi.org/10.1021/jp804045p

[40] **Barroso, M. M. (2011).** Quantum dots in Cell Biology. Journal of Histochemistry & Cytochemistry, 59(3), 237–251. https://doi.org/10.1369/0022155411398487

[41] **Williams, J. V., Kotov, N. A., & Savage, P. E. (2009).** A rapid hot-injection method for the improved hydrothermal synthesis of CdSe nanoparticles. Industrial & Engineering Chemistry Research, 48(9), 4316–4321. https://doi.org/10.1021/ie8007067

[42] **Mussa Farkhani, S., & Valizadeh, A. (2014).** Review: Three synthesis methods of cdx (X = se, s or Te) Quantum Dots. IET Nanobiotechnology, 8(2), 59–76. https://doi.org/10.1049/iet-nbt.2012.0028

[43] **Bertin, G., & Averbeck, D. (2006).** Cadmium: Cellular effects, modifications of biomolecules, modulation of DNA repair and genotoxic consequences (a review). Biochimie, 88(11), 1549–1559. https://doi.org/10.1016/j.biochi.2006.10.001

[44] **Hu, L., Zhong, H., & He, Z. (2021).** Toxicity evaluation of cadmium-containing Quantum Dots: A review of optimizing physicochemical properties to diminish toxicity. Colloids and Surfaces B: Biointerfaces, 200, 111609. https://doi.org/10.1016/j.colsurfb.2021.111609

[45] **D. Pan, Q. Wang, S. Jiang, X. Ji, L. An,** Low-temperature synthesis of oil-soluble CdSe, CdS, and CdSe/CdS core-shell nanocrystals by using various water-soluble anion precursors, J. Phys. Chem. C (2007), https://doi.org/10.1021/jp0678047.

[46] **Ünlü, C. (2019).** Controlling defect state emission in ultra-small sized tellurium doped CdSe nanocrystals via two-phase synthesis method. Optical Materials, 89, 361–367. https://doi.org/10.1016/j.optmat.2019.01.050

[47] **GÜLEROĞLU, G., & ÜNLÜ, C. (2021).** Spectroscopic investigation of defect-state emission in cdse quantum dots. TURKISH JOURNAL OF CHEMISTRY, 45(3), 520–527. https://doi.org/10.3906/kim-2101-66

[48] **Song, S. W., Lee, S. H., Jo, D. Y., Yoon, S. Y., Kim, H. M., Kim, Y., Han, J. N., Lee, Y. J., Do, Y. R., & Yang, H. (2021).** Single and dual doping of blue- emissive znsete quantum dots with transition metal ions. Advanced Optical Materials, 10(2), 2101767. https://doi.org/10.1002/adom.202101767

[49] **Jang, E.-P., Han, C.-Y., Lim, S.-W., Jo, J.-H., Jo, D.-Y., Lee, S.-H., Yoon, S.-Y., & Yang, H. (2019).** Synthesis of alloyed znsete quantum dots as bright, color-pure blue emitters. ACS Applied Materials & Interfaces, 11(49), 46062–46069. https://doi.org/10.1021/acsami.9b14763

[50] **Albani, J. R. (2004).** Fluorescence: Principles and Observables. Structure and Dynamics of Macromolecules: Absorption and Fluorescence Studies, 55–98. https://doi.org/10.1016/b978-044451449-3/50002-2

[51] **Daud, M. N., Zakaria, A., Jafari, A., Ghazali, M. S., Abdullah, W. R., & Zainal, Z. (2012).** Characterization of CdTe films deposited at various bath temperatures and concentrations using electrophoretic deposition. International Journal of Molecular Sciences, 13(5), 5706–5714. https://doi.org/10.3390/ijms13055706

[52] **Deng, Z., Yan, H., & Liu, Y. (2009).** Band Gap Engineering of Quaternary-alloyed zncdsse quantum dots via a facile phosphine-free colloidal method. Journal of the American Chemical Society, 131(49), 17744–17745. https://doi.org/10.1021/ja908408m

[53] **Bernard, J. E., & Zunger, A. (1986).** Optical bowing in zinc chalcogenide semiconductor alloys. Physical Review B, 34(8), 5992–5995. https://doi.org/10.1103/physrevb.34.5992

CURRICULUM VITAE

Name Surname **:** Merve ERKAN

EDUCATION:

- **B.Sc.** **:** 2019, Middle East Technical University, Faculty of Arts and Science, Chemistry
- **M.Sc** **:** 2023, Istanbul Technical University, Faculty of Arts and Science, Chemistry

PROFESSIONAL EXPERIENCE:

- 2022-Present Excelya: Sr. Assoc. Clinical Contracts and Budgets
- 2021-2022 Bilim Pharmaceutical: R&D Analytical Specialist
- 2020-2021 Bilim Pharmaceutical: R&D Analyst
- 2019-2020 Ali Raif Pharmaceutical: Quality Control Analyst

PUBLICATIONS, PRESENTATIONS:

- **Erkan, M.,** Ük, N., Nar, I., & Ünlü, C. (2023). Adapting two-phase synthesis method to develop cadmium poor Quaternary ZnCd-chalcogenide quantum dots. Optical Materials, 138, 113713. https://doi.org/10.1016/j.optmat.2023.113713
- **Erkan M.,** Development and Characterization of ZnCdSSe and CdSSeTe Quaternary Alloyed Quantum Dots. INTERNATIONAL GRADUATE RESEARCH SYMPOSIUM – IGRS 2022, Haziran 1-3, 2022 Istanbul Turkey
- Hacıefendioğlu, T., Solmaz, T. K., **Erkan, M.,** & Asil, D. (2020). A comprehensive approach for the instability of pbte quantum dots and design of a combinatorial passivation strategy. Solar Energy Materials and Solar Cells, 207, 110362. https://doi.org/10.1016/j.solmat.2019.110362